Molecular Therapy
Nucleic Acids
Original Article

Targeting Duchenne muscular dystrophy by skipping DMD exon 45 with base editors

Michael Gapinske,[1] Jackson Winter,[1] Devyani Swami,[1] Lauren Gapinske,[1,2] Wendy S. Woods,[1] Shraddha Shirguppe,[1] Angelo Miskalis,[1] Anna Busza,[1] Dana Joulani,[1] Collin J. Kao,[1] Kurt Kostan,[1] Anne Bigot,[3] Rashid Bashir,[1,2,4] and Pablo Perez-Pinera[1,4,5,6,7]

[1]Department of Bioengineering, University of Illinois at Urbana-Champaign, Urbana, IL 61801, USA; [2]Nick J. Holonyak Micro and Nano Technology Laboratory, University of Illinois at Urbana-Champaign, Urbana, IL 61801, USA; [3]Sorbonne Université, Inserm, Institut de Myologie, Centre de Recherche en Myologie, 75013 Paris, France; [4]Carle Illinois College of Medicine, Champaign, IL 61820, USA; [5]Carl R. Woese Institute for Genomic Biology, University of Illinois at Urbana-Champaign, Urbana, IL 61801, USA; [6]Cancer Center at Illinois, University of Illinois at Urbana-Champaign, Urbana, IL 61801, USA; [7]Department of Molecular and Integrative Physiology, University of Illinois Urbana-Champaign, Urbana, IL 61801, USA

Duchenne muscular dystrophy is an X-linked monogenic disease caused by mutations in the dystrophin gene (*DMD*) characterized by progressive muscle weakness, leading to loss of ambulation and decreased life expectancy. Since the current standard of care for Duchenne muscular dystrophy is to merely treat symptoms, there is a dire need for treatment modalities that can correct the underlying genetic mutations. While several gene replacement therapies are being explored in clinical trials, one emerging approach that can directly correct mutations in genomic DNA is base editing. We have recently developed CRISPR-SKIP, a base editing strategy to induce permanent exon skipping by introducing C > T or A > G mutations at splice acceptors in genomic DNA, which can be used therapeutically to recover dystrophin expression when a genomic deletion leads to an out-of-frame *DMD* transcript. We now demonstrate that CRISPR-SKIP can be adapted to correct some forms of Duchenne muscular dystrophy by disrupting the splice acceptor in human *DMD* exon 45 with high efficiency, which enables open reading frame recovery and restoration of dystrophin expression. We also demonstrate that AAV-delivered split-intein base editors edit the splice acceptor of *DMD* exon 45 in cultured human cells and *in vivo*, highlighting the therapeutic potential of this strategy.

INTRODUCTION

Duchenne muscular dystrophy is a degenerative disease of skeletal and cardiac muscle, caused by mutations in the dystrophin (*DMD*) gene. *DMD* encodes a protein that provides a stabilizing connection between the myocyte cytoskeleton and the dystroglycan complex, which serves as an anchor to the extracellular matrix.[1] Loss-of-function mutations in *DMD* destabilize the muscle membrane and lead to muscle cell deterioration, which is responsible for the symptoms of the disease and ultimately causes the death of the patients, typically in their 20s.[2] Because no curative therapy exists, the current standard of care for Duchenne muscular dystrophy is focused on symptomatic treatments.

More than 7,929 mutations have been reported in the *DMD* gene, more than 1,000 of which are associated with dystrophinopathies.[3,4] Mutations causing Duchenne muscular dystrophy are most common in mutational hotspots, particularly from exons 45 to 55.[5,6] For this reason, exon skipping therapies that exclude specific exons from mature transcripts can be used to restore dystrophin functionality for a large percentage of patients. Overall, exon skipping approaches targeting a single exon can be used to correct 60% of all Duchenne muscular dystrophy cases[3] and as many as 83% of all cases when one or two exons are skipped.[5]

In fact, an exon skipping therapy that uses antisense oligonucleotides (AONs), eteplirsen (Exondys 51), has been granted accelerated U.S. Food and Drug Administration (FDA) approval for treating patients with Duchenne muscular dystrophy mutations that can be addressed by skipping *DMD* exon 51.[7,8] A second exon skipping AON, casimersen (Amondys 45), has also recently been granted accelerated FDA approval for skipping *DMD* exon 45.[9] However, AONs have only a transient effect on RNA,[5,6,10–12] and thus necessitate repeated administration, which represents a life-long health care stressor on patients and hospitals, along with a large economic burden for some patients because of the high cost of these drugs.[8]

To overcome the limitations inherent to AON-based exon skipping approaches, gene editing technologies that alter the splicing of mutated *DMD* have been developed.[13–15] By directly modifying DNA, gene editing systems can accomplish permanent modifications leading to long-lasting therapeutic benefit after a single administration. CRISPR-Cas9, the most widely used gene editing platform, has been used to disrupt splice acceptor sequences, which induces exon skipping to recover dystrophin expression both in cells from

Received 15 December 2022; accepted 25 July 2023;
https://doi.org/10.1016/j.omtn.2023.07.029.

Correspondence: Pablo Perez-Pinera, Department of Bioengineering, University of Illinois at Urbana-Champaign, 1406 West Green Street, Urbana 61801-2910, USA.
E-mail: pablo@illinois.edu

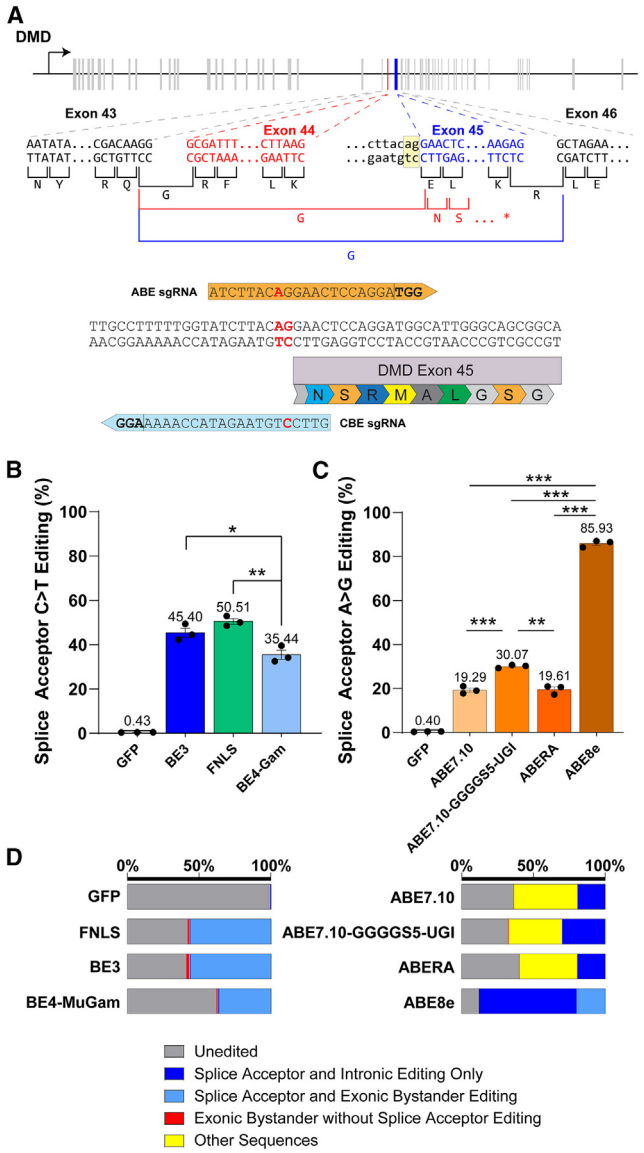

Figure 1. Base editing at *DMD* exon 45 in HEK293 cells

(A) Schematic representation of *DMD* splicing and the exon 45 splice acceptor. Wild-type exon splicing maintains the *DMD* open reading frame, but a deletion of exon 44 (red) causes a premature STOP codon in exon 45. Skipping exon 45 in cells with a deletion of exon 44 recovers the reading frame (blue). (B and C) Editing rates measured in HEK293T cells. Six days after transfection with a panel of (B) CBEs and (C) ABEs, editing in genomic DNA was quantified. Editing rates represented as mean ± s.d.; *p < 0.05; **p < 0.01; ***p < 0.001, two-tailed t tests; n = 3. (D) Graphical representation of base editing outcomes. Exonic bystander editing (light blue) was rare in the absence of splice acceptor editing (red).

patients with Duchenne muscular dystrophy[14–17] and in mouse models of Duchenne muscular dystrophy.[18–21]

However, CRISPR-Cas9 functions by inducing targeted double-strand breaks (DSB) in DNA and exon skipping with Cas9 relies on the error-prone non-homologous end-joining (NHEJ) DNA repair pathway to introduce a wide range of often undesirable mutations, some of which create splice-disrupting outcomes. Additionally, NHEJ repair can lead to unexpected mutations, chromosomal aberrations, chromothripsis, and DNA damage responses that can compromise the survival of the edited cells,[22–24] which has triggered the development of novel editing systems that can introduce targeted exon skipping more safely and precisely.

We previously overcame these problems by developing CRISPR-SKIP, a technology for disrupting the splice acceptor of target exons using Cas9 base editors (BEs).[25,26] CRISPR-SKIP relies on a Cas9 nickase fused with a deoxyadenosine or cytidine deaminase to precisely introduce A > G or C > T genomic DNA modifications, respectively, within splice acceptors without creating DSBs. The CRISPR-SKIP strategy was recently applied to skip exon 50 of the mouse *Dmd* gene, which was predicted to be applicable to ~4% of Duchenne muscular dystrophy cases if the results could be successfully translated to the human *DMD* exon 50.[3,27] In the current work, we first used CRISPR-SKIP with both cytidine- and adenine-BEs to effectively disrupt the splice acceptor of exon 45, which led to permanent exon skipping in cultured cells. We further demonstrated that split-intein BEs targeting *DMD* exon 45 are functional and can edit the *DMD* exon 45 splice acceptor after delivery by adeno-associated viral (AAV) vectors *in vitro* and *in vivo* via intramuscular or systemic injection, which, given the efficacy and safety profile of AAV, could enable application of this therapy to patients with Duchenne muscular dystrophy in the future.

Overall, this gene editing strategy could be used to treat ~9% of cases of Duchenne muscular dystrophy,[6] making it a substantial addition to the Duchenne muscular dystrophy therapeutic toolbox.

RESULTS

Characterization of on-target base editing activity

Since BEs can introduce targeted modifications in genomic DNA with higher precision and with a better safety profile than DSB-based gene editing tools, we first sought to identify the most active BE technologies for inducing skipping of exon 45 in *DMD* (Figure 1A). We previously demonstrated that exon skipping can be achieved by mutating splice acceptors with cytidine BEs (CBEs)[25] and adenine BEs (ABEs),[26] but there are multiple generations of each,[26,28–32] which have distinct editing preferences, specificity, editing windows, and bystander activity. For these reasons, we performed a CBE screening comparing the more conventional BE3[32] with BE4-Gam,[28] which generally increases base editing by approximately 50% over BE3 while decreasing the frequency of by-products, and that includes the bacteriophage Mu Gam protein for reducing indel formation, and FNLS,[29] which is a codon-optimized version of BE3 for efficient editing after delivery with lentiviral vectors (Figure 1B). The screening with ABEs included the first-generation ABE7.10,[31] ABE7.10 fused with a uracil glycosylase inhibitor (UGI),[26] which is generally more active than ABE7.10, ABERA,[29] a codon-optimized version of ABE7.10 for efficient editing after delivery with lentiviral vectors, and ABE8e,[30]

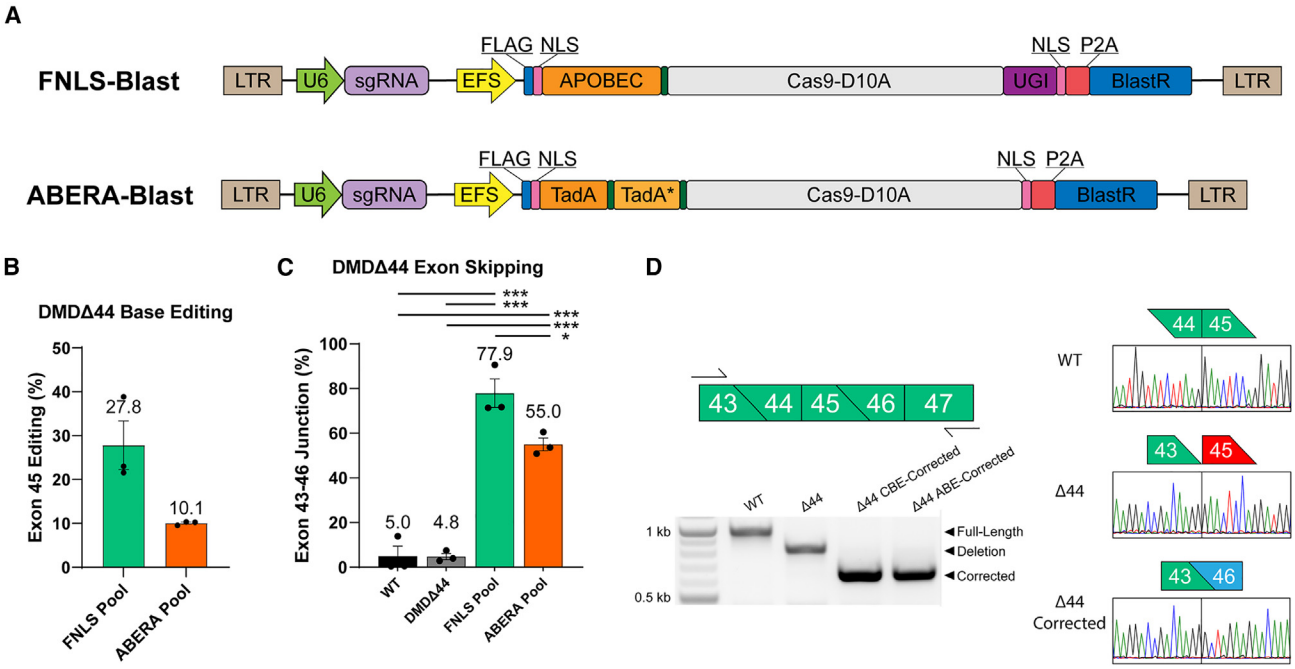

Figure 2. Lentiviral base editing and exon skipping in a human myoblast model of Duchenne muscular dystrophy

(A) Design of lentiviral expression cassettes to co-deliver a blasticidin-selectable CBE (FNLS-Blast) and ABE (ABERA-Blast) with a U6 sgRNA expression cassette. (B) NGS quantification of base editing rates achieved with lentiviral BEs post-selection. We measured C > T editing rates of 27.8% with FNLS-Blast, and an A > G editing rate of 10.1% with ABERA-Blast, n = 3. (C) Skipping of exon 45 was observed in 77.9% (FNLS-Blast) and 55% (ABERA-Blast) of reads from transcripts using the exon 44 splice donor. Editing rates represented as mean ± s.d.; *p < 0.05; ***p < 0.001, two-tailed t test; n = 3. (D) RT-PCR and Sanger sequencing of edited clonal cell lines generated from FNLS-Blast and ABERA-Blast selected pools.

which contains an engineered highly active adenosine deaminase (Figure 1C). Since in these experiments we exclusively used BEs built with SpCas9-D10A, which requires an NGG PAM, the splice acceptor of *DMD* exon 45 is within the editing window of only one CBE single guide RNA (sgRNA) and one ABE sgRNA. We transfected each BE-sgRNA pair in HEK293T cells by lipofection and analyzed mutations in genomic DNA via next-generation sequencing (NGS). In these experiments, the CBEs BE3 and FNLS introduced the highest modification rates at the target site (45.40% and 50.51%, respectively), while BE4-Gam was less effective (35.44%). When targeting the splice acceptor with ABEs, we observed that ABE8e had the greatest editing efficiency (85.93%), while ABE7.10-GGGGS5-UGI (30.07%) outperformed ABE7.10 and ABERA (19.29% and 19.61%, respectively). It should be noted that FNLS and ABERA used the EFS promoter and were codon optimized for increased expression levels while the other constructs used the CMV promoter and varied in their codon optimization schemes, which could partially account for some of the variance between the constructs.

Importantly, while CBEs and ABEs exhibited exonic bystander editing that would alter the amino acid sequence, it is predicted that exonic mutations that occur simultaneously with splice acceptor mutations would not have a biological effect since the exon would be skipped. We found that among all base editing outcomes, exonic base changes without splice acceptor mutations were relatively rare (Figure 1D). When using CBEs, the first base of *DMD* exon 45 was edited in nearly all reads that exhibited splice acceptor editing as well as an additional 1%–2% of reads. Similarly, no ABE construct caused more than 0.33% exonic bystander editing without a splice acceptor mutation, and ABE8e did not edit any exonic bystanders without also editing the splice acceptor. Overall, the results of these experiments identified a set of BE that can effectively disrupt the splice acceptor of *DMD* exon 45 with minimal bystander mutations.

Characterization of DMD exon 45 skipping by BEs

Next, we sought to characterize skipping of *DMD* exon 45 after genomic DNA editing. Since HEK293T cells do not express dystrophin, we created a human myoblast Duchenne muscular dystrophy cell line with a deletion of exon 44 (DMDΔ44) to determine if splice acceptor editing would cause therapeutic exon skipping (Materials and methods) (Figure S1). To ensure efficient gene delivery in our DMDΔ44 myoblast cell line, we chose to use lentiviral delivery of BEs and sgRNAs. To facilitate delivery of BEs and sgRNAs, we modified the FNLS (CBE) and ABERA (ABE) lentiviral BE vectors to contain a U6-sgRNA expression cassette and a blasticidin resistance gene tethered to the BEs via a P2A sequence (FNLS-Blast, ABERA-Blast) (Figure 2A). While FNLS and ABERA were not the most active BEs at this target site in transient transfections, they were extensively codon optimized, including removal of polyadenylation sites within the cDNA, for efficient expression and activity after lentiviral

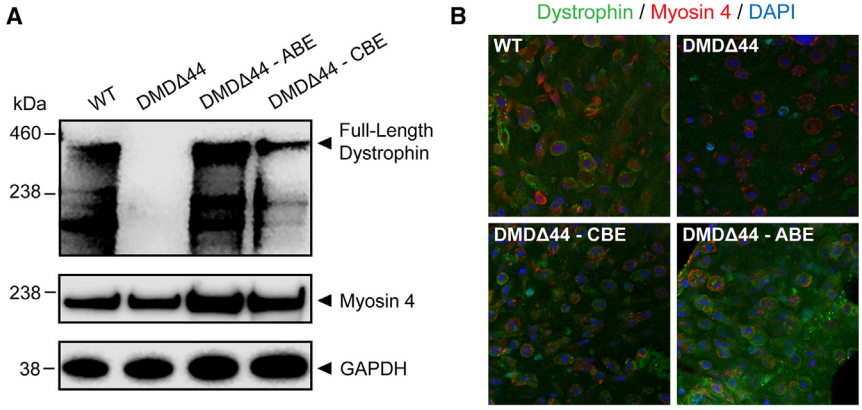

Figure 3. Recovery of dystrophin expression following base editing

(A) Detection of dystrophin and myosin-4 from differentiated WT, DMDΔ44, and base-edited myoblast cell lines by western blot. (B) Detection of dystrophin by immunofluorescence imaging of myotube cross-sections. Representative immunofluorescent images stained with DAPI (blue), rabbit anti-Dystrophin (green), and MF20 (red) to label mature myotubes are shown.

transduction. For this reason, we chose them to generate clonal cell lines by viral transduction. We transduced the DMDΔ44 myoblast cell line with FNLS-Blast or ABERA-Blast, we applied selection with blasticidin, and pooled cells were differentiated into skeletal muscle myotubes for 5 days. After differentiation, we measured DNA editing rates and *DMD* exon 45 skipping using NGS and found that FNLS-Blast and ABERA-Blast edited the splice acceptor in 27.8% and 10.1% of reads, respectively (Figure 2B). To fully characterize the spectrum of splice alterations introduced by base editing and check for the usage of cryptic splice acceptors, we performed NGS from mRNA from exons 43 to 47. We found that FNLS-Blast caused an exon skipping rate of 77.9%, while ABERA-Blast editing led to an exon skipping rate of 55.0% (Figure 2C). Because exon skipping is required to recover the *DMD* reading frame in DMDΔ44 cells, we hypothesize that nonsense mediated mRNA decay contributed to the high exon skipping rates observed relative to editing rates, as the corrected transcripts are expected to have much longer half-lives than the mutant transcripts, which are more rapidly degraded.[33] Furthermore, it should be noted that PCR bias toward the smaller transcripts missing both exons 44 and 45 instead of just exon 44 could also contribute to high skipping rates relative to DNA editing. Importantly, we also determined by NGS that our DMDΔ44 disease model did not undergo alternative splicing of the exon 43-exon 46 junction to recover the *DMD* reading frame without BE activity. Finally, NGS of pooled ABERA-Blast-edited cells revealed only 0.16% inclusion of exonic bystander editing, causing a silent mutation in the mature mRNA, which further emphasizes that bystander exonic editing is not a concern when it occurs simultaneously with splice acceptor editing (Figure S2).

To better understand the splice patterns of edited cells, we isolated clonal cell lines with the splice acceptor edited by FNLS-Blast or ABERA-Blast. Each isolated clone also carried a bystander mutation, which was intronic for ABERA-Blast and exonic for FNLS-Blast. RT-PCR and Sanger sequencing showed that the frameshift-correcting exon 43-46 junction was the most common *DMD* isoform (Figure 2D). While NGS showed that the FNLS-corrected clonal cell line used the exon 43-exon 46 in-frame splice junction in more than 99% of transcripts, the ABERA-corrected cell line used the 43-exon 46 in-frame splice junction in more than 97.4% of transcripts and a cryptic splice acceptor within exon 45 in 2.3% of transcripts (Figure S3). This alternative splice event does not recover the DMDΔ44 reading frame and is, therefore, not therapeutic. However, given the rarity of this splice event compared to exon 45 skipping, we do not anticipate the existence of this splice event to be detrimental to the therapeutic goal of treating Duchenne muscular dystrophy via CRISPR-SKIP.

Analysis of dystrophin protein expression

We next used the BE-corrected cell lines to determine whether skipping exon 45 restored dystrophin expression, which is drastically decreased following deletion of exon 44 in comparison with wild-type myoblasts. The clonal cell populations were differentiated into skeletal muscle myotubes and after 7 days the expression of dystrophin was analyzed by western blot probed with an anti-dystrophin antibody, anti-MF20, and anti-GAPDH antibodies. Analysis of cell lysates by western blot demonstrated that skipping of exon 45 in DMDΔ44 cells successfully restored dystrophin protein expression (Figure 3A).

Additionally, we created muscle tissue constructs from wild-type myoblasts, DMDΔ44 myoblasts, and DMDΔ44 myoblasts treated with CBEs or ABEs following previously published protocols that enable three-dimensional formation of contractile muscle tissue that can be sectioned to ascertain expression and subcellular localization of dystrophin.[34] Immunohistochemical staining with an antibody raised against the C-terminal domain of dystrophin (ab15277, Abcam) demonstrated that in wild-type myotubes dystrophin is localized primarily to the cell membrane, while in DMDΔ44 myoblasts dystrophin is absent. Treatment with exon 45-skipping CBEs or ABEs restored expression of dystrophin, which was observed at the plasma membrane, as well as in the cytoplasm (Figure 3B).

AAV-mediated CRISPR-SKIP for DMD exon 45

Given its efficacy and safety profile, AAV is rapidly becoming the platform of choice for *in vivo* gene delivery.[35] However, AAV vectors have limited packaging capacity, which makes them incompatible with large DNA cargoes, such as transgenes encoding BEs. To overcome this problem, we recently engineered a split-intein BE technology in which the N-terminus of the BE, including a nuclear localization signal, the deaminase domain, the first 712 amino acids of

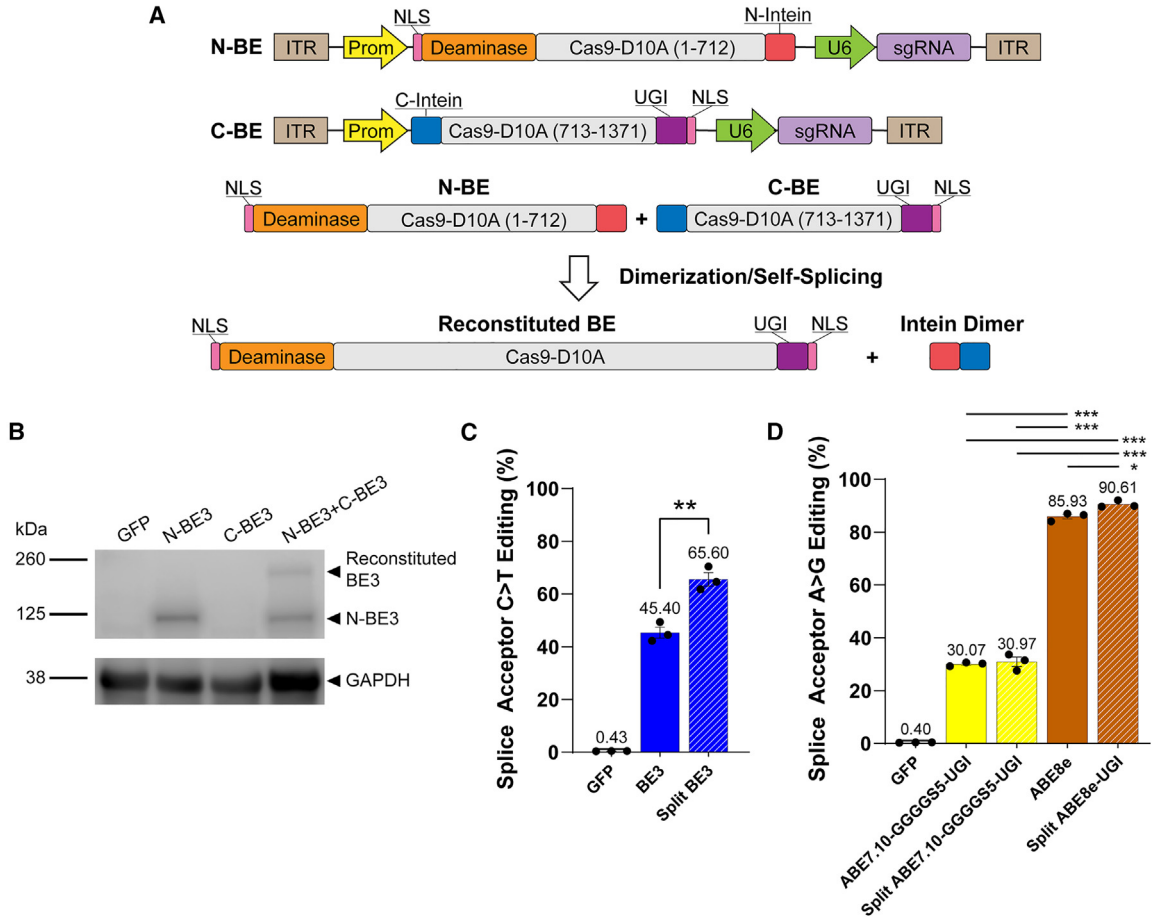

Figure 4. Split BE Constructs for Editing Exon 45 Splice Acceptor

(A) Design of split BE constructs and schematic representation of their intein-based reconstitution upon co-delivery. (B) Western blot showing reconstitution of the full-length BE3, using an antibody directed to an N-terminal V5 epitope tag. (C and D) Base editing rates achieved by split BEs were equivalent to (ABE7.10-GGGS5-UGI) or surpassed (BE3, ABE8e) the editing rates achieved with full-length BEs. Editing rates represented as mean ± s.d.; *p < 0.05; **p < 0.01; ***p < 0.001, two-tailed t test; n = 3.

SpCas9-D10A are fused with the N-terminal *Rhodothermus marinus* DnaB split intein.[26,36] A second vector contains the DNA sequences encoding the C-terminal split intein, SpCas9 amino acids 713–1371, the UGI domain, and an NLS. A U6-sgRNA expression cassette is also included in each vector (Figure 4A). We packaged the split base editing system into AAV, used the viral particles to transduce HEK293T cells and demonstrated reconstitution of the full-length BE after transduction using western blot with anti-V5 antibodies (Figure 4B).

We tested our split-BE platform by editing the splice acceptor of *DMD* exon 45 in HEK293T cells with a split-BE3, split-ABE7.10-GGGGS5-UGI, and split-ABE8e-UGI and found that each BE showed editing rates comparable or greater than to its full-length counterpart (Figures 4C and 4D). While we did not directly compare the editing rates of ABE8e with or without a UGI domain, our previously published results[26] and the data shown in Figure 1 support that it generally enhances the activity of ABEs and, for this reason, we elected to include it in the split-intein AAV vectors. Additionally, one important consideration when using BEs is their potential for off-target editing.[25,37] To determine the off-target editing rates of our split BEs split-BE3 and split-ABE8e-UGI, we performed NGS sequencing at predicted off-target loci from split BE-transfected HEK293T cells.

We found significant off-target editing at three loci when using split-CBE (30.7%, 25.1%, and 0.69%), though notably no editing was observed in coding regions. We did not detect off-target editing at the loci tested when using ABE8e-UGI (Figure S4 and Table S1).

In vivo Dmd exon 45 editing

We next tested the ability of CRISPR-SKIP to edit the splice acceptor of mouse *Dmd* exon 45 *in vivo* after delivery by AAV. Given the sequence differences between the human and mouse genomes at the splice acceptor site (Figure 5A), we determined that using a truncated sgRNA with full homology to both the human and mouse genome would give us the best estimate of the therapeutic potential of CRISPR-SKIP to

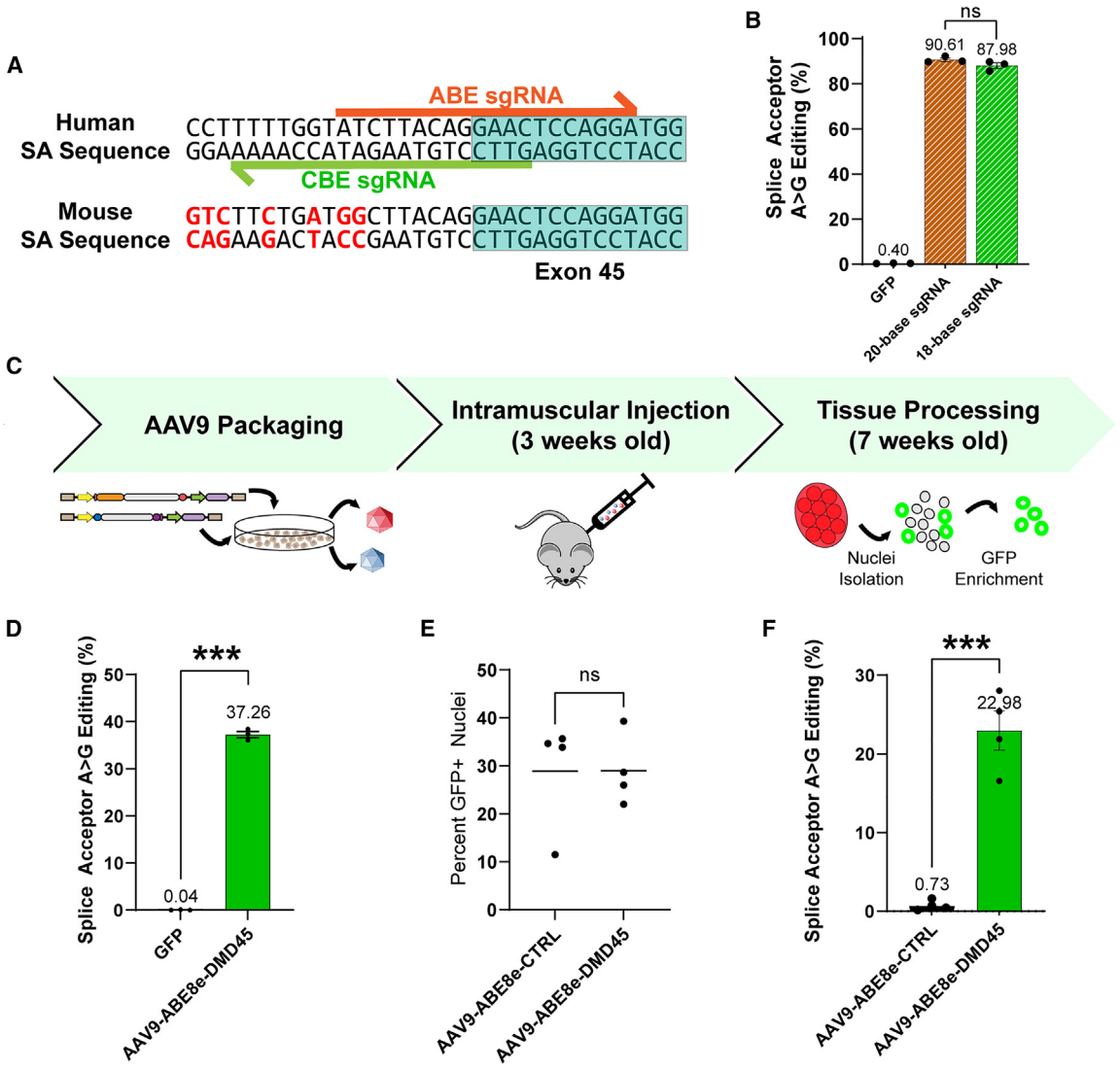

Figure 5. *In vivo* editing of the splice acceptor of *Dmd* exon 45

(A) Alignment of mouse and human dystrophin gene sequences. Human and mouse exon 45 splice acceptor sequences allow for each to be targeted with the same sgRNA only if an 18-nucleotide spacer is used with an ABE. (B) Editing rates in HEK293T cells treated with split-ABE8e-UGI and either an sgRNA with a 20-nucleotide spacer (90.61%) or with an 18-nucleotide spacer (87.98%); n=3. (C) Schematic of workflow for testing *in vivo* editing. Viral vectors were packaged into AAV9 capsids using HEK293T cells and purified. Male mice were injected with 1E11 VG of each split BE construct and 1E10 VG of GFP-KASH intramuscularly into the biceps femoris. After 4 weeks, nuclei were isolated and GFP+ nuclei were enriched using FACS followed by analysis of DNA editing rates by NGS. (D) AAV transduction of HEK293T cells. HEK293T cells transduced with AAV9-ABE8e-DMD45 exhibited 37.26% editing of the splice acceptor; n = 3. (E) Comparison of transduction efficiency following injection of the targeting or non-targeting BEs. No significant difference was seen between the percent of GFP+ nuclei in mice injected with the BE and an sgRNA targeting the Rosa26 safe-harbor locus; n = 4. (F) Base editing rates following intramuscular injection of the targeting or non-targeting BEs. 22.98% A > G base editing was accomplished in mice injected with the split-ABE8e-UGI AAV targeted to *Dmd* exon 45; n=4. Editing rates represented as mean ± s.d.; ns, $p > 0.05$; ***$p < 0.001$; two-tailed t test.

effectively edit the splice acceptor of *Dmd* exon 45. In these experiments we used ABE8e, which edits the splice acceptor of human *DMD* exon 45 with the highest efficiency (Figure 1C). First, we demonstrated that in HEK293T cells there is no significant difference between the editing rates of split-ABE8e-UGI used in conjunction with an sgRNA with a 20-nucleotide spacer or with a 5′-truncated 18-nucleotide spacer with full homology to both the human and mouse sequences (Figure 5B). Interestingly, while ABE8e-UGI did not install off-target mutations when using a 20-nucleotide sgRNA spacer (Figure S4 and Table S1), we observed off-target editing at 4 sites when using an 18-nucleotide sgRNA spacer (Figure S5 and Table S1).

Next, we packaged split-ABE8e-UGI with the sgRNA with an 18-nucleotide truncated spacer or a control sgRNA into AAV9 capsids,

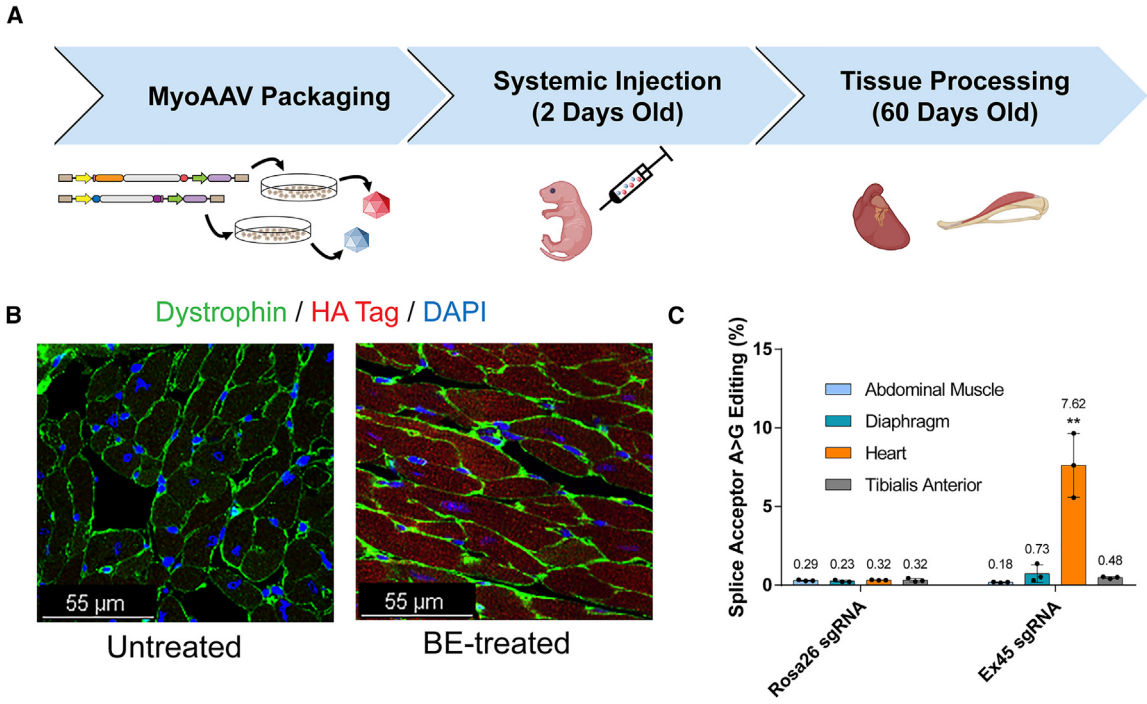

Figure 6. Base editing of the *Dmd* exon 45 splice acceptor following systemic delivery by AAV

(A) Schematic of workflow for systemic injection of AAV. Viral vectors were packaged into MyoAAV capsids using HEK293T cells and purified. Two-day-old male C57BL/6J mice were injected systemically via facial vein injection with 5E10 VG of each BE construct. Four weeks after injection, tissue from the abdominal muscle, diaphragm, heart, and tibialis anterior were collected and processed for sequencing of genomic DNA and immunohistochemistry experiments. (B) Immunohistochemical analysis of cardiac muscle after AAV injection. Immunohistochemistry of control uninjected mice (left panel) and mice injected with BEs staining for the HA tag fused to the C-terminus of the BE (red), dystrophin (green) and DAPI (blue) shows expression of BE in the heart. Scale bar, 55 µm. (C) Quantification of *in vivo* base editing in genomic DNA by NGS in mice injected with split-ABE8e-UGI AAV. Editing rates represented as mean ± s.d.; $^{**}p < 0.01$; two-tailed t test; n = 3.

to make AAV9-ABE8e-DMD45 and AAV9-ABE8e-CTRL, respectively (Figure 5C). We delivered each BE vector to HEK293T cells at an estimated MOI of 2.5E5 vector genomes per cell to confirm that the AAV-delivered split-ABE8e-UGI would edit human cells and found a 37.26% editing rate at the splice acceptor of *DMD* exon 45 (Figure 5D).

We next delivered 2E11 vector genomes of AAV9-ABE8e-DMD45 or AAV9-ABE8e-CTRL along with 1E10 vector genomes of AAV9-GFP-Klarsicht/ANC-1/Syne-1 homology (KASH) per mouse via intramuscular injection in the biceps femoris of male C57BL/6J mice (Figure 5C). AAV9-GFP-KASH contained a payload of GFP fused to the KASH nuclear membrane localization domain, which was used to label nuclei of successfully transduced myotubes. Four weeks after injection, we isolated nuclei from the injected muscle and used fluorescence-activated cell sorting (FACS) to enrich for GFP-positive nuclei and found no significant difference in the percent of GFP-positive nuclei in mice injected with AAV9-ABE8e-DMD45 and AAV9-ABE8e-CTRL (Figure 5E). We analyzed editing rates of the GFP-KASH-enriched nuclei via NGS and found an A > G editing rate at the target site of 22.98% (Figure 5F).

Finally, we sought to evaluate the efficacy of our base editing system when delivered systemically via MyoAAV, a recently engineered AAV capsid containing an RGD peptide that offers enhanced transduction efficiencies to muscle cells compared with other serotypes.[38] We packaged split-ABE8e-UGI and the sgRNA with an 18-nucleotide spacer or a Rosa26 targeting control sgRNA into MyoAAV and injected 5E10 vector genomes (VG) of each BE vector systemically into 2-day-old mice via facial vein injection. At 60 days post-injection, we harvested tissue from the abdominal muscle, diaphragm, heart, and tibialis anterior for analysis of editing rates in genomic DNA by NGS and BE distribution using immunohistochemistry (Figure 6A).

We performed immunohistochemistry staining with anti-HA antibodies to detect the C-terminal tag of the split-ABE8e-UGI construct, which confirmed the presence of the BE in the cytoplasm of cardiomyocytes. We observed low levels of expression of the BE in most cells, but the levels of expression were variable with some cells expressing high levels of BE (Figure 6B). While no measurable editing was detected in the abdominal muscle compared with control mice, we observed editing in the tibialis anterior and diaphragm, although this was not statistically significant because of variability across mice (Figure 6C). We did, however, observe significant editing in the cardiac muscle with a maximum of 9.7% in one mouse and a mean editing rate of 7.62%.

DISCUSSION

In this work, we developed a base editing system to edit the splice acceptor of *DMD* exon 45 both *in vitro* and *in vivo*, as well as to induce skipping of exon 45 of human *DMD in vitro*. Exon 45 is a hotspot for mutations in the *DMD* gene that cause Duchenne muscular dystrophy, thus skipping exon 45 is a potential therapeutic approach which could potentially correct ~9% of Duchenne muscular dystrophy cases. Importantly, AONs for inducing skipping of *DMD* exon 45 have recently received FDA accelerated approval (Sarepta, ClinicalTrials.gov ID: NCT02500381) for the treatment of patients with Duchenne muscular dystrophy amenable to exon 45 skipping, although the clinical benefit remains to be established.[9,39] Given the transient nature and rapid clearance of AON therapies, this therapeutic modality requires repeated administration of the AON, with limited activity in the periods of time leading up to the new dosage.

Alternatively, most existing gene editing approaches to correct Duchenne muscular dystrophy-causing mutations rely on the use of active nucleases to delete specific exons or introduce DSBs at splice acceptors to restore the reading frame of *DMD*.[14,15,18–20] While these approaches have been successful at restoring the expression of internally truncated forms of dystrophin, a major limitation of this approach is the unpredictability of the mutations introduced, which could potentially create novel and unexpected variants of unknown biological significance, activate and select for mutations in the p53 pathway,[22,40–42] as well as lead to chromosomal translocations or chromothripsis.[22–24]

To overcome these problems, in this work we adapted CRISPR-SKIP to induce skipping of exon 45 of the *DMD* gene and restore dystrophin expression using BEs. Base editing-mediated correction directly edits the genome and since BEs do not introduce DSBs in DNA, their safety profile is better than that of CRISPR systems that utilize active nucleases.

The strategy of skipping *DMD* exon 45 is applicable to multiple Duchenne muscular dystrophy deletion patterns, including deletions of exons 44, 46–47, 46–48, 46–49, 46–51, and 46–53, and the exon skipping outcomes of each of these mutations may vary, based on the stability and folding of the internally-truncated protein product.[6,43,44] Notably, the outcome of skipping exon 45 in the presence of an exon 44 deletion is the exon 44–45 Becker muscular dystrophy deletion, which is not commonly reported[44] perhaps because it is associated with a phenotype that is very mild and not well characterized.

To evaluate the therapeutic potential of base editing with regards to Duchenne muscular dystrophy by skipping exon 45, we first demonstrated that the single-base editing approach restores dystrophin expression in human myotubes with a deletion of exon 44 in the *DMD* gene. We demonstrated that a CBE-edited clonal cell line skipped exon 45 in more than 99% of reads, while our ABE-edited clonal cell line also included a nine-base partial skip of exon 45 in 2.3% of reads, which does not recover the reading frame of Duchenne muscular dystrophy mutations, though this did not seem to have a significant effect on protein expression. It is important to note that exon skipping can also be achieved by mutating the conserved GT dinucleotide found immediately downstream of the targeted exon.[45–48] Targeting splice donors has been shown to reduce partial exon skipping by avoiding activation of cryptic splice acceptors, although it can lead to partial or full intron retention, which can potentially disrupt the reading frame and function of the resulting transcripts. While the lack of an appropriately positioned NGG PAM sequence prevented us from targeting the splice donor sequence of DMD exon 45 with the set of editing tools we used, BEs with relaxed PAM requirements such as SpCas9-NG[49] and SpCas9-SpRY[50] could be used to target the splice donor of exon 45 for comprehensive evaluation of splicing outcomes.

Interestingly, we observed by immunofluorescence that while dystrophin was localized primarily at the sarcolemma as expected, the edited clones exhibited more cytoplasmic localization than wild-type cells. The unexpected subcellular localization of dystrophin in this experimental setting could be the result of different levels of differentiation of the different tissue constructs, given that during differentiation of skeletal muscle dystrophin is first localized in the cytoplasm.[51]

Two main concerns when using BEs are bystander mutations and off-target effects. Since BEs can edit all available base pairs within a defined editing window, they have the potential to generate bystander edits that are deleterious in some gene editing applications. However, CRISPR-SKIP applications are unique in that bystander modifications that occur in conjunction with splice acceptor editing would not affect the coding sequence, as any exonic mutations would be skipped with the remainder of the exon.

We observed off-target editing with both cytidine and ABEs. Interestingly, the split-ABE8e-UGI with a truncated 18-nucleotide sgRNA spacer exhibited significantly higher off-target editing than the full-length ABE8e with a 20-nucleotide sgRNA spacer, although they have similar on-target editing rates, which suggests that the additional length of this 20-nucleotide sgRNA spacer enhances specificity of ABE8e (Figures 5B, S4, and S5). Importantly, all the off-target mutations detected occurred in non-coding regions of the genome and are unlikely to be biologically relevant, although OT5 for the 18-base pair ABE sgRNA introduced a mutation within a non-coding RNA, long non-coding RNA SGO1-AS1, which may warrant follow-up investigation. Despite the low off-target editing with 20-base pair sgRNAs, off-target editing remains a concern because BEs also exhibit RNA editing that is independent of sgRNA sequence, and cannot be predicted effectively with current technologies.[52–54]

AAV is a promising gene therapy delivery tool that provides long-term expression of transgenes *in vivo*.[55,56] While the size of BEs exceeds the packaging capacity of single AAV particles, we and others

have previously demonstrated that split-intein BEs can be used to effectively deliver active BEs *in vivo* via AAV.[26,27,36,57,58]

In this study, we demonstrated base editing *in vivo* in C57BL/6J mice, which express wild-type dystrophin. Given the similarity between human and mouse dystrophin, this model enabled demonstration of the feasibility of *in vivo* editing of *Dmd*, however this mutation is predicted to result in skipping of exon 45 in wild-type dystrophin and an early stop codon, which prevents the detection of exon skipping. Additional studies in humanized mouse models with human *DMD* lacking exon 44 will be critical to further establish the therapeutic value of this approach. Notably, because skeletal muscle is multinucleated, a given myotube could have a combination of both edited and unedited nuclei and few edited nuclei within a myotube could compensate for lack of dystrophin expression by unedited nuclei, thereby leading to recovery of *DMD* protein in a larger proportion of myotubes than what the editing rates alone would suggest. Since we observed that 98% of mRNA transcripts from our ABE-edited DMDΔ44 model cell line exhibit exon skipping, we expect dystrophin expression to be recovered in any myotube containing an edited nucleus. Since recovery of as little as ∼4% of dystrophin expression has been demonstrated to drastically improve Duchenne muscular dystrophy phenotype in animal models,[59] the 23% editing rate we achieved through intramuscular injection has potential therapeutic value, although it should be noted that these editing rates were accomplished through injection of an AAV dosage higher than the maximum dose recommended by the FDA (3E14 VG/kg) when adjusted to the estimated weight of the biceps femoris muscle.

Because DMD is a systemic neuromuscular disease, we sought to investigate editing outcomes after systemic injection of AAV into 2-day-old mouse neonates. To facilitate systemic delivery of AAV to muscles, several groups have engineered AAV capsids to have enhanced muscle tropism through directed evolution[38,60,61] or rational engineering of surface-exposed regions of the capsid proteins to cells with or without lower liver retention.[62–64] We used one of these evolved AAV variants with improved muscle transduction, MyoAAV,[38] to systemically deliver our base editing system. While we detected very limited editing in the diaphragm, abdominal muscle or tibialis anterior of the injected pups, we did observe significant DNA editing in the heart tissue with values of up to 9.7% in one mouse. Successful cardiac editing is particularly promising as patients with Duchenne muscular dystrophy typically succumb to heart or respiratory failure. The low levels of editing at the other muscle groups could be attributed to the titer of 2.5E13 VG/kg, an order of magnitude lower than the dosages used in current clinical trials for Duchenne muscular dystrophy.[65]

The only *DMD* gene editing approach to date that explored *DMD* reframing strategies without DSBs targeted exon 50 of the mouse *Dmd* gene with CRISPR-SKIP and exon 52 of the human *DMD* gene with prime editors.[27] In addition to reframing strategies to correct whole-exon deletions in *DMD*, CRISPR-SKIP has also been used to skip a mutation-containing exon that is a multiple of three base pairs,[46] thereby eliminating the mutation from the transcripts without altering the reading frame. We anticipate that similar approaches can be developed to target other mutational hotspots within *DMD* to further expand the potential for base editing technologies to provide therapeutic options for most patients with Duchenne muscular dystrophy.

In summary, the work described in this paper demonstrate that both cytidine and ABEs can recover expression of the dystrophin protein in a model of Duchenne muscular dystrophy using a single base change to disrupt a splice acceptor, leading to exon skipping and reading frame correction. Since permanent modification of genomic DNA is advantageous over the transient effect of AONs and base editing induces permanent changes in genomic DNA without relying on potentially deleterious DSBs, the strategy described in this work with further optimization has potential for therapeutic impact.

MATERIALS AND METHODS

Cell culture and transfection

The cell line HEK293T was obtained from the American Type Culture Collection and was maintained in DMEM supplemented with 10% fetal bovine serum and 1% penicillin/streptomycin at 37°C with 5% CO_2. For BE characterization, HEK293T cells were transfected in 24-well plates with Lipofectamine 2000 (Invitrogen) following the manufacturer's instructions. The amount of DNA used for lipofection was 1 μg per well. Transfection efficiency was routinely higher than 90% for 293T cells as determined by fluorescent microscopy after delivery of a control GFP expression plasmid.

The cell line AB1190c16 was a gift from Vincent Mouly and was maintained in Skeletal Muscle Complete Growth Media (SMCGM) (PromoCell C-23060) supplemented with Growth Media Supplement Mix (PromoCell C-39365), 15% fetal bovine serum, and 1% penicillin/streptomycin) at 37°C with 5% CO_2.

Model cell line generation

We chose AB1190c16—an immortalized myoblast cell line from an apparently healthy male—as the parent cell line because it can be effectively differentiated into dystrophin-expressing skeletal muscle myotubes. To create our disease model cell line, we used NAVI[66,67] to first integrate a plasmid within *DMD* exon 44 and then used a two-sgRNA deletion approach to remove the plasmid and the exon. To generate the DMDΔ44 cell line, 250,000 AB1190c16 cells were electroporated with SpCas9 (Addgene, #41815), pCMV-GFP-T2A-HygroR, a plasmid expressing a transfer vector sgRNA, and a plasmid expressing a *DMD* exon 44-targeting sgRNA. Electroporations were performed using a Bio-Rad GenePulser Xcell (square wave, 160 V, 950 μF, infinite resistance, 0.2 cm cuvette; Bio-Rad), and after 1 week of recovery cells were selected with 250 μg/mL hygromycin (GoldBio). A clonal cell line with a vector integration in *DMD* exon 44 was isolated and integration was confirmed by PCR using the KAPA2G Robust PCR kit (Roche) according to manufacturer's

instructions. The cell line was again electroporated with SpCas9 and two sgRNA vectors targeting introns 43 and 44. GFP-negative cells were sorted using FACS (Roy J Carver Biotechnology Center, Cytometry and Microscopy to Omics, UIUC), and a clonal cell line with a deletion of exon 44 was isolated, expanded, and genetically characterized by PCR using the KAPA2G Robust PCR kit (Roche) according to manufacturer's instructions.

Plasmids and cloning

The plasmids encoding SpCas9 (#41815), BE3 (#73021), BE4-Gam (#100806), FNLS (#211476), ABE8e (#138489), ABERA (#215671), and the U6-sgRNA expression cassette (#47108) were obtained from Addgene. SgRNAs were cloned into the sgRNA plasmid backbone with paired oligonucleotides (IDT, Table S2) as previously described.[67] Briefly, the oligonucleotides used to create the guide sequences were hybridized, phosphorylated and cloned into the sgRNA vector using BpiI (ThermoFisher), or into AAV vectors using BsaI-HFv2 (NEB), T4-PNK (NEB), and T4 DNA Ligase (NEB).

The ABE7.10 plasmid was previously cloned through Gibson assembly of a gBlock Gene Fragment (IDT) and an SpCas9-D10A backbone (Addgene #41816).[26] The ABE7.10-GGGGS5-UGI plasmid was previously cloned through sequential Gibson assembly of the SpCas9-D10A backbone, a gBlock (IDT), and a PCR product generated from the BE3 plasmid (#73021) (Table S3).

The pCMV-GFP-T2A-HygroR transfer vector plasmid was previously cloned with gBlock gene fragments obtained from IDT into the pCDNA3.1 backbone[66] (Table S3).

The lentiviral expression plasmids pLenti-EFS-FNLS-P2A-BlastR (FNLS-Blast) and pLenti-EFS-ABERA-P2A-BlastR (ABERA-Blast) were cloned using pLenti-FNLS-P2A-GFP-PGK-Puro (Addgene #211476) and pLenti-ABERA-P2A-Puro (Addgene #215671). pLenti-FNLS-P2A-GFP-PGK-Puro was digested with NheI and XbaI (NEB), pLenti-ABERA-P2A-Puro was digested with NheI and MluI (NEB), and a P2A-BlastR gene was inserted after amplification by KAPA HiFi HotStart PCR kit and purification on a DNA Clean and Concentrator column (Zymo Research) (Table S4). Subsequently, the U6-sgRNA expression cassette was cloned into the lentiviral plasmids upstream of the promoter at the XhoI (NEB) restriction site, via Gibson assembly with Kapa HiFi HotStart PCR amplicons generated from the sgRNA expression cassette plasmid.

The AAV plasmids were cloned by Gibson assembly using gBlocks (IDT) encoding the split BE sequences and U6 expression cassettes with a CMV promoter, using the NotI and XbaI restriction sites of pX602 (Addgene #107055) (Table S5).

Lentiviral vector production

For lentiviral vector production, HEK293T cells were seeded in 10-cm dishes 15–18 h before transfection of 20 μg lentiviral vector, 20 μg packaging plasmid (psPAX2, Addgene #12260), and 5 μg lentiviral envelope plasmid (psMD2.G, Addgene #12259). The plasmid DNA was mixed with 0.25 M $CaCl_2$, and 2× HEPES-buffered saline was added dropwise while vortexing. The resultant DNA-calcium phosphate precipitate was added to adherent HEK293T cells at 80%–90% confluence. After 24 h, the cell media was discarded and replaced. Viral supernatant was collected every 24 h for the next 72 h, filtered with 0.45-μm syringe filters (Sigma-Aldrich), concentrated ∼30× using 100-kDa filter units (Amicon), mixed with an appropriate volume of SMCGM, and 4 μg/mL polybrene was added. We resuspended 250,000 DMDΔ44 cells in the viral media and plated in 6-well plates.

Three-dimensional skeletal muscle tissue fabrication and imaging

Skeletal muscle tissues were formed by resuspending 1E7 myoblast cells/mL within a matrix mixture of 30% v/v Matrigel (BD Biosciences), 4 mg/mL fibrinogen (Sigma-Aldrich), and 0.5 U/mg fibrinogen thrombin (Sigma-Aldrich) in SMCGM supplemented with 1 mg/mL aminocaproic acid (ACA, Sigma-Aldrich). The cell-matrix suspension was pipetted into an injection mold formed of 20% w/v polyethylene glycol diacrylate (Sigma-Aldrich) of molecular weight 700 g/mol with 0.1% w/v lithium phenyl-2,4,6-trimethylbenzoylphosphinate (Sigma-Aldrich) photoinitiator, and 0.04% w/v Sunset Yellow FCF (Sigma-Aldrich). Molds were printed three-dimensionally using the Asiga PICO2 printer, with two pillars to serve as anchors for muscle tissue attachment. After 3 days in cell growth media supplemented with ACA, cell differentiation was initiated by switching to DMEM supplemented with 5% horse serum, 1% insulin-transferrin-selenium mix, and 1 mg/mL ACA. Tissues were differentiated for 7 days before collection.

Immunofluorescence imaging of *in vitro* tissues

After 1 week of differentiation, tissues were fixed in 4% paraformaldehyde (Sigma-Aldrich), permeabilized with 0.1% Triton X-100 (Sigma-Aldrich) and blocked using 3% w/v bovine serum albumin (Sigma-Aldrich) in PBS-T (PBS with 0.1% v/v Tween 20). Tissues were embedded in 3% agarose and sliced with a vibratome at a thickness of 300 μm. Tissues were labeled with rabbit anti-dystrophin (ab15277, 1:200, AbCam), mouse anti-myosin 4 (MF20, 1:200, ThermoFisher) and 4′,6-Diamidino-2-Phenylindole (DAPI, 1 μg/mL, Sigma-Aldrich). Fluorescent images were taken using a multiphoton confocal microscope (LSM 710, Carl Zeiss).

AAV vector production

AAV was produced as previously described.[68] pAAV2/9n was a gift from James M. Wilson (Addgene plasmid # 112865). The RGD peptide described by Tabebordbar et al. was cloned into the pAAV2/9n backbone to create pMyoAAV through Gibson assembly using a gBlock gene fragment (IDT).[38] pJEP317-pAAV-U6SaCas9gRNA (SapI)-EFS-GFP-KASH-pA was a gift from Jonathan Ploski (Addgene plasmid # 113694) and was modified through removal of the U6 sgRNA expression cassette and exchange of the EFS promoter with a CMV promoter through Gibson assembly to create pAAV-GFP-KASH. pHelper was purchased from Cell Biolabs Inc.

HEK293T cells were seeded onto 15-cm plates to be 80% confluent after 16 h and maintained in DMEM supplemented with 10% (v/v) FBS and 1% (v/v) penicillin/streptomycin. After 16 h, cells were transfected with 65 μg total of AAV vector plasmid (pAAV-CMV-N-ABE8e-DMD45, pAAV-CMV-C-ABE8e-UGI-DMD45, or pAAV-GFP-KASH), pAAV2/9n or pMyoAAV, and pHelper in a 1:1:1 molar ratio using $CaPO_4$ precipitation. XmaI digestion was used to confirm the integrity of the pAAV plasmids before transfection. Cells were harvested 72 h after transfection by manual dissociation using a cell scraper and centrifuged at 500×*g* for 5 min at room temperature. Cells were then resuspended in 2 mL per plate of Lysis Buffer (50 mM Tris-HCl and 150 mM NaCl, pH 8.0) with 0.5% Triton X-100 (Sigma-Aldrich), frozen in liquid nitrogen and thawed in a 37°C water bath for three freeze-thaw cycles. Cell lysates were incubated with 10 U Benzonase (Sigma-Aldrich)/mL of cell lysate for 30 min at 37°C. We then centrifuged the lysate at 10,000×*g* for 15 min at room temperature. The resulting supernatant was overlaid onto an iodixanol density gradient, and viral vectors were isolated by ultracentrifugation at 42,000 RPM at 18°C. After extraction, AAV was filter-dialyzed three times with 15 mL PBS with 0.001% Tween 20 using an Ultra-15 Centrifugal Filter Unit (Amicon) at 3,000×*g* and concentrated to 2 mL. Viral vectors were stored at 4°C and the genomic titer was determined by quantitative real-time PCR using SsoFast Evagreen (Bio-Rad).

Injections

All animal procedures were approved by the Institutional Animal Care and Use Committee at the University of Illinois and conducted in accordance with the National Institutes of Health Guide for the Care and Use of Laboratory Animals. Intramuscular injections of 3-week-old male C57Bl/6J mice (Jackson Laboratory #000664) were performed by injecting 1×10^{11} VG each of AAV9-CMV-N-ABE8e-DMD45 and AAV9-CMV-C-ABE8e-UGI-DMD45 and 1×10^{10} VG of AAV9-GFP-KASH in 100 μL of PBS with 0.001% Tween 20 into the right biceps femoris using a 0.3-mL insulin syringe (BD). Systemic injections of 2-day-old male C57Bl/6J neonates was performed by injecting 5×10^{10} VG each of MyoAAV-CMV-N-ABE8e-DMD45 and MyoAAV-CMV-C-ABE8e-UGI-DMD45 in 50 μL PBS with 0.001% Tween 20 using a 3/10 mL insulin syringe with 3/8″ 30G needle.

NGS

DNA amplicons for NGS were generated by PCR using KAPA HiFi HotStart (Roche), according to manufacturer's instructions, using primers with overhangs compatible with Nextera XT indexing (IDT, Table S2). After validation of the quality of PCR products by gel electrophoresis, the PCR products were isolated using an AMPure XP PCR purification beads (Beckman Coulter). Indexed amplicons were then generated using a Nextera XT DNA Library Prep Kit (Illumina) quantitated, and pooled. Libraries were sequenced with a MiSeq Nano Flow Cell for 251 cycles from each end of the fragment using a MiSeq Reagent Kit v2 (500 cycles). FASTQ files were created and demultiplexed using bcl2fastq v2.17.1.14 Conversion Software (Illumina). Deep sequencing was performed by the Roy J. Carver Biotechnology Center at the University of Illinois, Urbana, Illinois. Base editing rates were quantified using CRISPResso2.[69] Reads with average phred scores below 30 were removed, and remaining reads were aligned to the expected amplicon sequences.

Exon skipping rates were quantified by NGS, using the STAR RNA-Seq aligner.[70] After cDNA synthesis (qScript, QuantaBio), amplicons were generated using KAPA HiFi HotStart, purified as described, and sequenced with MiSeq Bulk Flow Cell for 301 cycles from each end of the fragment using a MiSeq Reagent Kit v3 (600-cycles). Resulting reads were demultiplexed and aligned to the human genome (GRCh38) using STAR, with "–clip3pNbases" set to 100 for reads from cells with exon 44 deleted.[70] Splice junction usage was determined from STAR SJ.out.tab files and the exon 45 skipping rate for each sample was defined as the number of reads using the exon 46 splice acceptor divided by the total number of reads using the exon 44 splice donor (WT cells) or the exon 43 splice donor (DMDΔ44 and corrected cell lines). Bystander editing in cDNA was determined using BAM files that were aligned, sorted, and indexed by STAR with the Integrative Genomics Viewer's (IGV's) igvtools count function with window size set to 1, minimum mapping quality set to 30, and the "-bases" setting on.[71]

Western blot

Cells were lysed using RIPA buffer (10 mM Tris-HCl, 140 mM NaCl, 1 mM EDTA, 1% Triton X-100, 0.1% SDS, and 0.5% sodium deoxycholate, 2.5% beta-mercaptoethanol, pH 8.0). Protein concentrations were determined using a Pierce BCA Protein Assay Kit (ThermoFisher Cat. 23225) according to manufacturer's instructions. For dystrophin and myosin-4 staining, 5 μg total protein was loaded into NuPage Tris-Acetate gels and run for 90 min at 130 V in NuPage Tris-Acetate SDS running buffer (Invitrogen). For GAPDH staining, 1 μg total protein was loaded into NuPage 4%–12% Bis-Tris gels and was run for 50 min at 200 V in NuPage MES SDS running buffer (Invitrogen). Transfer to nitrocellulose membranes was performed in Towbin's transfer buffer (20 mM Tris-HCl, 150 mM glycine, and 10% [v/v] methanol) for 1.5 h at 100 V. Membranes were blocked with 5% (v/v) bovine serum albumin fraction V or 5% (w/v) nonfat dry milk in Tris-buffered saline (TBS) (20 mM Tris-HCl, 150 mM NaCl, and 0.1%, pH 7.5) with 1% Tween 20 (TBS-T) for 1 h and then incubated overnight at 4°C with primary antibodies in blocking solution. The following primary antibodies were used: mouse anti-dystrophin (1:1000; Sigma-Aldrich, MANDYS8), mouse anti-myosin-4 (1:500; ThermoFisher, MF20), rabbit anti-V5 (1:1000; Cell Signaling Technology, 13202S), and rabbit anti-GAPDH (1:1,000; Cell Signaling Technology, 2118S). After the overnight incubation, membranes were washed three times with TBS-T and incubated with goat anti-rabbit or horse anti-mouse horseradish peroxidase conjugated antibodies (1:10,000; Cell Signaling Technology, 7074P2, 7076P2) in blocking solution for 1 h at room temperature. Membranes were washed three times with TBS-T and developed using Clarity Western ECL Substrate (Bio-Rad) and visualized by automated chemiluminescence using a Licor Odyssey imager.

Nuclei isolation

Nuclei were isolated from tissue as previously described.[72] Briefly, harvested muscle was first homogenized in 2 mL of Nuclei EZ Lysis Buffer (Sigma-Aldrich) using the KIMBLE Dounce Tissue Grinder (Sigma-Aldrich) per the manufacturer's instructions. After the addition of an extra 2 mL of Nuclei EZ Lysis Buffer to each homogenized tissue, samples were incubated at room temperature (RT) for 5 min. Homogenized tissues were then centrifuged at 500×*g* for 5 min. After removing the supernatant, nuclei were resuspended in 4 mL of Nuclei Suspension Buffer (PBS with 100 μg/mL BSA and 3.33 μM Vibrant Dye Cycle Violet Stain; ThermoFisher Scientific). Nuclei were centrifuged at 500×*g* for 1 min and resuspended in 1 mL of Nuclei Suspension Buffer for FACS.

FACS

Harvested cells or nuclei were strained using a 35 μm filter and sorted using a BD FACSAria II Cell Sorter (Roy J. Carver Biotechnology Center, University of Illinois, Urbana, IL). Cells were collected in PureLink RNA Mini Kit Lysis Buffer (Invitrogen) or DNeasy Blood & Tissue Kit Lysis Buffer (Qiagen). At least 15,000 cells or nuclei were sorted for each sample.

Immunohistochemistry of mouse tissues

Harvested muscle tissue was fixed in 4% paraformaldehyde overnight at 4°C. Fixed tissues were then cut to 16-μm sagittal sections using a CM3050 S cryostat (Leica) and stored in cryoprotectant at −20°C. Before staining, sections were washed with PBS three times for 15 min and incubated in permeabilization buffer 0.5% Triton X-100 for 45 min and later incubated in blocking solution (PBS with 10% [v/v] Goat serum; Abcam) for 30 min at RT. Sections were then stained with primary antibodies in blocking solution overnight at 4°C. After incubation, sections were washed three times with PBS and incubated with secondary antibodies for 1 h at RT. Sections were then washed three times. Cell Nuclei were stained using DAPI and sections were mounted onto slides using VECTASHIELD HardSet Antifade Mounting Medium (Vector Laboratories). Sections were imaged using a Leica TCS SP8 confocal microscope (Beckman Institute Imaging Technology Microscopy Suite, University of Illinois, Urbana, IL).

The following primary antibodies were used: rabbit anti-HA (1:100; Cell Signaling Technology, 3724S) mouse monoclonal anti-Dystrophin antibody MANDYS8 (1:200, Signa Aldrich, D8168). The following secondary antibodies were used: goat anti-rabbit Alexa Fluor 555 (1:400, Cell Signaling Technology 4413), and donkey anti-mouse Alexa Fluor 488 (1:400, Abcam 150113).

Statistical analysis

Statistical analysis was performed using GraphPad Prism 8. DNA editing data were analyzed by two-tailed unpaired t test and represented as mean ± s.d.

DATA AND CODE AVAILABILITY

All data necessary to evaluate the conclusions is presented within the manuscript or in supplemental information. Deep sequencing files have been deposited in the Gene Expression Omnibus, accession number GSE235673.

SUPPLEMENTAL INFORMATION

Supplemental information can be found online at https://doi.org/10.1016/j.omtn.2023.07.029.

ACKNOWLEDGMENTS

We thank the DNA Services staff of the Roy J. Carver Biotechnology Center at the University of Illinois, particularly Alvaro Hernandez and Chris Wright, for their support with DNA and RNA sequencing. We thank Basia Balhan of the Roy J. Carver Biotechnology Center Cytometry and Microscopy to Omics facility at the University of Illinois for her support with FACS. This work was supported by the National Institutes of Health (1U01NS122102, 1R01NS123556, 1R01GM141296, 1R01GM127497, and 1R01GM131272), the Muscular Dystrophy Association (MDA602798), the American Heart Association (17SDG33650087), and the National Science Foundation (1735252). M.G. was supported by the GRFP program from the National Science Foundation (DGE – 1746047). J.W was supported by the Northwestern University Clinical and Translational Science Institute, grant UL1TR001422. A.M was supported by the National Institute of Biomedical Imaging and Bioengineering of the National Institutes of Health under Award Number T32EB019944. The content is solely the responsibility of the authors and does not necessarily represent the official views of the National Institutes of Health.

AUTHOR CONTRIBUTIONS

M.G. and P.P. conceived of the study; A.B. provided critical reagents; M.G., J.W., D.S., L.G., W.S.W., S.S., A.M., A.B., D.J., C.J.K., K.K., R.B., and P.P., designed and performed experiments; M.G., J.W., and P.P. wrote the manuscript with input from all authors.

DECLARATION OF INTERESTS

The authors have filed patent applications on CRISPR technologies.

REFERENCES

1. Blake, D.J., Weir, A., Newey, S.E., and Davies, K.E. (2002). Function and Genetics of Dystrophin and Dystrophin-Related Proteins in Muscle. Physiol. Rev. *82*, 291–329. https://doi.org/10.1152/PHYSREV.00028.2001.

2. Fairclough, R.J., Wood, M.J., and Davies, K.E. (2013). Therapy for Duchenne muscular dystrophy: Renewed optimism from genetic approaches. Nat. Rev. Genet. *14*, 373–378. https://doi.org/10.1038/nrg3460.

3. Flanigan, K.M., Dunn, D.M., Von Niederhausern, A., Soltanzadeh, P., Gappmaier, E., Howard, M.T., Sampson, J.B., Mendell, J.R., Wall, C., King, W.M., et al. (2009). Mutational spectrum of DMD mutations in dystrophinopathy patients: Application of modern diagnostic techniques to a large cohort. Hum. Mutat. *30*, 1657–1666. https://doi.org/10.1002/humu.21114.

4. Aartsma-Rus, A., Van Deutekom, J.C.T., Fokkema, I.F., Van Ommen, G.J.B., and Den Dunnen, J.T. (2006). Entries in the Leiden Duchenne muscular dystrophy mutation database: An overview of mutation types and paradoxical cases that confirm the reading-frame rule. Muscle Nerve *34*, 135–144. https://doi.org/10.1002/mus.20586.

5. Aartsma-Rus, A., Fokkema, I., Verschuuren, J., Ginjaar, I., van Deutekom, J., van Ommen, G.-J., and den Dunnen, J.T. (2009). Theoretic applicability of antisense-mediated exon skipping for Duchenne muscular dystrophy mutations. Hum. Mutat. *30*, 293–299. https://doi.org/10.1002/humu.20918.

6. Nakamura, A. (2017). Moving towards successful exon-skipping therapy for Duchenne muscular dystrophy. J. Hum. Genet. *62*, 871–876. https://doi.org/10.1038/jhg.2017.57.

7. Syed, Y.Y. (2016). Eteplirsen: First Global Approval. Drugs *76*, 1699–1704. https://doi.org/10.1007/s40265-016-0657-1.

8. McNally, E.M., and Wyatt, E.J. (2017). Mutation-based therapy for duchenne muscular dystrophy: Antisense treatment arrives in the clinic. Circulation *136*, 979–981. https://doi.org/10.1161/CIRCULATIONAHA.117.028382.

9. Shirley, M. (2021). Casimersen: First Approval. Drugs *81*, 875–879. https://doi.org/10.1007/S40265-021-01512-2.

10. Kole, R., and Krieg, A.M. (2015). Exon skipping therapy for Duchenne muscular dystrophy. Adv. Drug Deliv. Rev. *87*, 104–107. https://doi.org/10.1016/j.addr.2015.05.008.

11. Cirak, S., Arechavala-Gomeza, V., Guglieri, M., Feng, L., Torelli, S., Anthony, K., Abbs, S., Garralda, M.E., Bourke, J., Wells, D.J., et al. (2011). Exon skipping and dystrophin restoration in patients with Duchenne muscular dystrophy after systemic phosphorodiamidate morpholino oligomer treatment: An open-label, phase 2, dose-escalation study. Lancet *378*, 595–605. https://doi.org/10.1016/S0140-6736(11)60756-3.

12. Aartsma-Rus, A., and Van Ommen, G.J.B. (2007). Antisense-mediated exon skipping: A versatile tool with therapeutic and research applications. RNA *13*, 1609–1624. https://doi.org/10.1261/rna.653607.

13. Ousterout, D.G., Perez-Pinera, P., Thakore, P.I., Kabadi, A.M., Brown, M.T., Qin, X., Fedrigo, O., Mouly, V., Tremblay, J.P., and Gersbach, C.A. (2013). Reading frame correction by targeted genome editing restores dystrophin expression in cells from duchenne muscular dystrophy patients. Mol. Ther. *21*, 1718–1726. https://doi.org/10.1038/mt.2013.111.

14. Long, C., Li, H., Tiburcy, M., Rodriguez-Caycedo, C., Kyrychenko, V., Zhou, H., Zhang, Y., Min, Y.L., Shelton, J.M., Mammen, P.P.A., et al. (2018). Correction of diverse muscular dystrophy mutations in human engineered heart muscle by single-site genome editing. Sci. Adv. *4*, eaap9004. https://doi.org/10.1126/sciadv.aap9004.

15. Zhang, Y., Long, C., Bassel-Duby, R., and Olson, E.N. (2018). Myoediting: Toward prevention of muscular dystrophy by therapeutic genome editing. Physiol. Rev. *98*, 1205–1240. https://doi.org/10.1152/physrev.00046.2017.

16. Li, H.L., Fujimoto, N., Sasakawa, N., Shirai, S., Ohkame, T., Sakuma, T., Tanaka, M., Amano, N., Watanabe, A., Sakurai, H., et al. (2015). Precise Correction of the Dystrophin Gene in Duchenne Muscular Dystrophy Patient Induced Pluripotent Stem Cells by TALEN and CRISPR-Cas9. Stem Cell Rep. *4*, 143–154. https://doi.org/10.1016/J.STEMCR.2014.10.013.

17. Maggio, I., Stefanucci, L., Janssen, J.M., Liu, J., Chen, X., Mouly, V., and Gonçalves, M.A.F.V. (2016). Selection-free gene repair after adenoviral vector transduction of designer nucleases: rescue of dystrophin synthesis in DMD muscle cell populations. Nucleic Acids Res. *44*, 1449–1470. https://doi.org/10.1093/NAR/GKV1540.

18. Nelson, C.E., Hakim, C.H., Ousterout, D.G., Thakore, P.I., Moreb, E.A., Castellanos Rivera, R.M., Madhavan, S., Pan, X., Ran, F.A., Yan, W.X., et al. (2016). In vivo genome editing improves muscle function in a mouse model of Duchenne muscular dystrophy. Science *351*, 403–407. https://doi.org/10.1126/science.aad5143.

19. Min, Y.L., Chemello, F., Li, H., Rodriguez-Caycedo, C., Sanchez-Ortiz, E., Mireault, A.A., McAnally, J.R., Shelton, J.M., Zhang, Y., Bassel-Duby, R., and Olson, E.N. (2020). Correction of Three Prominent Mutations in Mouse and Human Models of Duchenne Muscular Dystrophy by Single-Cut Genome Editing. Mol. Ther. *28*, 2044–2055. https://doi.org/10.1016/j.ymthe.2020.05.024.

20. Amoasii, L., Long, C., Li, H., Mireault, A.A., Shelton, J.M., Sanchez-Ortiz, E., McAnally, J.R., Bhattacharyya, S., Schmidt, F., Grimm, D., et al. (2017). Single-cut genome editing restores dystrophin expression in a new mouse model of muscular dystrophy. Sci. Transl. Med. *9*, eaan8081. https://doi.org/10.1126/scitranslmed.aan8081.

21. Long, C., Amoasii, L., Mireault, A.A., McAnally, J.R., Li, H., Sanchez-Ortiz, E., Bhattacharyya, S., Shelton, J.M., Bassel-Duby, R., and Olson, E.N. (2016). Postnatal genome editing partially restores dystrophin expression in a mouse model of muscular dystrophy. Science *351*, 400–403. https://doi.org/10.1126/science.aad5725.

22. Cullot, G., Boutin, J., Toutain, J., Prat, F., Pennamen, P., Rooryck, C., Teichmann, M., Rousseau, E., Lamrissi-Garcia, I., Guyonnet-Duperat, V., et al. (2019). CRISPR-Cas9 genome editing induces megabase-scale chromosomal truncations. Nat. Commun. *10*, 1136–1214. https://doi.org/10.1038/s41467-019-09006-2.

23. Adikusuma, F., Piltz, S., Corbett, M.A., Turvey, M., McColl, S.R., Helbig, K.J., Beard, M.R., Hughes, J., Pomerantz, R.T., and Thomas, P.Q. (2018). Large deletions induced by Cas9 cleavage. Nature *560*, E8–E9. https://doi.org/10.1038/s41586-018-0380-z.

24. Leibowitz, M.L., Papathanasiou, S., Doerfler, P.A., Blaine, L.J., Sun, L., Yao, Y., Zhang, C.-Z., Weiss, M.J., and Pellman, D. (2021). Chromothripsis as an on-target consequence of CRISPR–Cas9 genome editing. Nat. Genet. *53*, 895–905. https://doi.org/10.1038/s41588-021-00838-7.

25. Gapinske, M., Luu, A., Winter, J., Woods, W.S., Kostan, K.A., Shiva, N., Song, J.S., and Perez-Pinera, P. (2018). CRISPR-SKIP: Programmable gene splicing with single base editors. Genome Biol. *19*, 107–111. https://doi.org/10.1186/s13059-018-1482-5.

26. Winter, J., Luu, A., Gapinske, M., Manandhar, S., Shirguppe, S., Woods, W.S., Song, J.S., and Perez-Pinera, P. (2019). Targeted exon skipping with AAV-mediated split adenine base editors. Cell Discov. *5*, 41. https://doi.org/10.1038/s41421-019-0109-7.

27. Chemello, F., Chai, A.C., Li, H., Rodriguez-Caycedo, C., Sanchez-Ortiz, E., Atmanli, A., Mireault, A.A., Liu, N., Bassel-Duby, R., and Olson, E.N. (2021). Precise correction of Duchenne muscular dystrophy exon deletion mutations by base and prime editing. Sci. Adv. *7*, eabg4910. https://doi.org/10.1126/SCIADV.ABG4910.

28. Komor, A.C., Zhao, K.T., Packer, M.S., Gaudelli, N.M., Waterbury, A.L., Koblan, L.W., Kim, Y.B., Badran, A.H., and Liu, D.R. (2017). Improved base excision repair inhibition and bacteriophage Mu Gam protein yields C:G-to-T:A base editors with higher efficiency and product purity. Sci. Adv. *3*, eaao4774. https://doi.org/10.1126/sciadv.aao4774.

29. Zafra, M.P., Schatoff, E.M., Katti, A., Foronda, M., Breinig, M., Schweitzer, A.Y., Simon, A., Han, T., Goswami, S., Montgomery, E., et al. (2018). Optimized base editors enable efficient editing in cells, organoids and mice. Nat. Biotechnol. *36*, 888–893. https://doi.org/10.1038/nbt.4194.

30. Richter, M.F., Zhao, K.T., Eton, E., Lapinaite, A., Newby, G.A., Thuronyi, B.W., Wilson, C., Koblan, L.W., Zeng, J., Bauer, D.E., et al. (2020). Phage-assisted evolution of an adenine base editor with improved Cas domain compatibility and activity. Nat. Biotechnol. *38*, 883–891. https://doi.org/10.1038/s41587-020-0453-z.

31. Gaudelli, N.M., Komor, A.C., Rees, H.A., Packer, M.S., Badran, A.H., Bryson, D.I., and Liu, D.R. (2017). Programmable base editing of A-T to G-C in genomic DNA without DNA cleavage. Nature *551*, 464–471. https://doi.org/10.1038/nature24644.

32. Komor, A.C., Kim, Y.B., Packer, M.S., Zuris, J.A., and Liu, D.R. (2016). Programmable editing of a target base in genomic DNA without double-stranded DNA cleavage. Nature *533*, 420–424. https://doi.org/10.1038/nature17946.

33. Chang, Y.F., Imam, J.S., and Wilkinson, M.F. (2007). The Nonsense-Mediated Decay RNA Surveillance Pathway. Annu. Rev. Biochem. *76*, 51–74. https://doi.org/10.1146/ANNUREV.BIOCHEM.76.050106.093909.

34. Raman, R., Grant, L., Seo, Y., Cvetkovic, C., Gapinske, M., Palasz, A., Dabbous, H., Kong, H., Pinera, P.P., and Bashir, R. (2017). Damage, Healing, and Remodeling in Optogenetic Skeletal Muscle Bioactuators. Adv. Healthc. Mater. *6*, 1700030. https://doi.org/10.1002/adhm.201700030.

35. Naso, M.F., Tomkowicz, B., Perry, W.L., and Strohl, W.R. (2017). Adeno-Associated Virus (AAV) as a Vector for Gene Therapy. BioDrugs *31*, 317–334. https://doi.org/10.1007/s40259-017-0234-5.

36. Lim, C.K.W., Gapinske, M., Brooks, A.K., Woods, W.S., Powell, J.E., Zeballos C, M.A., Winter, J., Perez-Pinera, P., Gaj, T., and Gaj, T. (2020). Treatment of a Mouse Model of ALS by In Vivo Base Editing. Mol. Ther. *28*, 1177–1189. https://doi.org/10.1016/j.ymthe.2020.01.005.

37. Rees, H.A., Komor, A.C., Yeh, W.H., Caetano-Lopes, J., Warman, M., Edge, A.S.B., and Liu, D.R. (2017). Improving the DNA specificity and applicability of base editing

through protein engineering and protein delivery. Nat. Commun. *8*, 15790. https://doi.org/10.1038/ncomms15790.

38. Tabebordbar, M., Lagerborg, K.A., Stanton, A., King, E.M., Ye, S., Tellez, L., Krunnfusz, A., Tavakoli, S., Widrick, J.J., Messemer, K.A., et al. (2021). Directed evolution of a family of AAV capsid variants enabling potent muscle-directed gene delivery across species. Cell *184*, 4919–4938.e22. https://doi.org/10.1016/J.CELL.2021.08.028.

39. Wagner, K.R., Kuntz, N.L., Koenig, E., East, L., Upadhyay, S., Han, B., and Shieh, P.B. (2021). Safety, tolerability, and pharmacokinetics of casimersen in patients with Duchenne muscular dystrophy amenable to exon 45 skipping: A randomized, double-blind, placebo-controlled, dose-titration trial. Muscle Nerve *64*, 285–292. https://doi.org/10.1002/MUS.27347.

40. Ihry, R.J., Worringer, K.A., Salick, M.R., Frias, E., Ho, D., Theriault, K., Kommineni, S., Chen, J., Sondey, M., Ye, C., et al. (2018). P53 inhibits CRISPR-Cas9 engineering in human pluripotent stem cells. Nat. Med. *24*, 939–946. https://doi.org/10.1038/s41591-018-0050-6.

41. Haapaniemi, E., Botla, S., Persson, J., Schmierer, B., and Taipale, J. (2018). CRISPR-Cas9 genome editing induces a p53-mediated DNA damage response. Nat. Med. *24*, 927–930. https://doi.org/10.1038/s41591-018-0049-z.

42. Enache, O.M., Rendo, V., Abdusamad, M., Lam, D., Davison, D., Pal, S., Currimjee, N., Hess, J., Pantel, S., Nag, A., et al. (2020). Cas9 activates the p53 pathway and selects for p53-inactivating mutations. Nat. Genet. *52*, 662–668. https://doi.org/10.1038/s41588-020-0623-4.

43. Anthony, K., Arechavala-Gomeza, V., Ricotti, V., Torelli, S., Feng, L., Janghra, N., Tasca, G., Guglieri, M., Barresi, R., Armaroli, A., et al. (2014). Biochemical characterization of patients with in-frame or out-of-frame DMD deletions pertinent to exon 44 or 45 skipping. JAMA Neurol. *71*, 32–40. https://doi.org/10.1001/jamaneurol.2013.4908.

44. Findlay, A.R., Wein, N., Kaminoh, Y., Taylor, L.E., Dunn, D.M., Mendell, J.R., King, W.M., Pestronk, A., Florence, J.M., Mathews, K.D., et al. (2015). Clinical phenotypes as predictors of the outcome of skipping around DMD exon 45. Ann. Neurol. *77*, 668–674. https://doi.org/10.1002/ANA.24365.

45. Yuan, J., Ma, Y., Huang, T., Chen, Y., Peng, Y., Li, B., Li, J., Zhang, Y., Song, B., Sun, X., et al. (2018). Genetic Modulation of RNA Splicing with a CRISPR-Guided Cytidine Deaminase. Mol. Cell. *72*, 380–394.e7. https://doi.org/10.1016/j.molcel.2018.09.002.

46. Li, J., Wang, K., Zhang, Y., Qi, T., Yuan, J., Zhang, L., Qiu, H., Wang, J., Yang, H.-T., Dai, Y., et al. (2021). Therapeutic Exon Skipping Through a CRISPR-Guided Cytidine Deaminase Rescues Dystrophic Cardiomyopathy in Vivo. Circulation *144*, 1760–1776. https://doi.org/10.1161/circulationaha.121.054628.

47. Chai, A.C., Chemello, F., Li, H., Nishiyama, T., Chen, K., Zhang, Y., Sánchez-Ortiz, E., Alomar, A., Xu, L., Liu, N., et al. (2023). Single-swap editing for the correction of common Duchenne muscular dystrophy mutations. Mol. Ther. Nucleic Acids *32*, 522–535. https://doi.org/10.1016/j.omtn.2023.04.009.

48. Musunuru, K., Chadwick, A.C., Mizoguchi, T., Garcia, S.P., DeNizio, J.E., Reiss, C.W., Wang, K., Iyer, S., Dutta, C., Clendaniel, V., et al. (2021). In vivo CRISPR base editing of PCSK9 durably lowers cholesterol in primates. Natalia *593*, 429–434. https://doi.org/10.1038/s41586-021-03534-y.

49. Nishimasu, H., Shi, X., Ishiguro, S., Gao, L., Hirano, S., Okazaki, S., Noda, T., Abudayyeh, O.O., Gootenberg, J.S., Mori, H., et al. (2018). Engineered CRISPR-Cas9 nuclease with expanded targeting space. Science *361*, 1259–1262. https://doi.org/10.1126/science.aas9129.

50. Walton, R.T., Christie, K.A., Whittaker, M.N., and Kleinstiver, B.P. (2020). Unconstrained genome targeting with near-PAMless engineered CRISPR-Cas9 variants. Science *368*, 290–296. https://doi.org/10.1126/science.aba8853.

51. Chevron, M.P., Girard, F., Claustres, M., and Demaille, J. (1994). Expression and subcellular localization of dystrophin in skeletal, cardiac and smooth muscles during the human development. Neuromuscul. Disord. *4*, 419–432. https://doi.org/10.1016/0960-8966(94)90081-7.

52. Zuo, E., Sun, Y., Wei, W., Yuan, T., Ying, W., Sun, H., Yuan, L., Steinmetz, L.M., Li, Y., and Yang, H. (2019). Cytosine base editor generates substantial off-target single-nucleotide variants in mouse embryos. Science *364*, 289–292. https://doi.org/10.1126/SCIENCE.AAV9973.

53. Yu, Y., Leete, T.C., Born, D.A., Young, L., Barrera, L.A., Lee, S.J., Rees, H.A., Ciaramella, G., and Gaudelli, N.M. (2020). Cytosine base editors with minimized unguided DNA and RNA off-target events and high on-target activity. Nat. Commun. *11*, 2052–2110. https://doi.org/10.1038/s41467-020-15887-5.

54. Gaudelli, N.M., Lam, D.K., Rees, H.A., Solá-Esteves, N.M., Barrera, L.A., Born, D.A., Edwards, A., Gehrke, J.M., Lee, S.J., Liquori, A.J., et al. (2020). Directed evolution of adenine base editors with increased activity and therapeutic application. Nat. Biotechnol. *38*, 892–900. https://doi.org/10.1038/s41587-020-0491-6.

55. Daya, S., and Berns, K.I. (2008). Gene Therapy Using Adeno-Associated Virus Vectors. Clin. Microbiol. Rev. *21*, 583–593. https://doi.org/10.1128/CMR.00008-08.

56. Penaud-Budloo, M., Le Guiner, C., Nowrouzi, A., Toromanoff, A., Chérel, Y., Chenuaud, P., Schmidt, M., von Kalle, C., Rolling, F., Moullier, P., and Snyder, R.O. (2008). Adeno-Associated Virus Vector Genomes Persist as Episomal Chromatin in Primate Muscle. J. Virol. *82*, 7875–7885. https://doi.org/10.1128/JVI.00649-08.

57. Levy, J.M., Yeh, W.H., Pendse, N., Davis, J.R., Hennessey, E., Butcher, R., Koblan, L.W., Comander, J., Liu, Q., and Liu, D.R. (2020). Cytosine and adenine base editing of the brain, liver, retina, heart and skeletal muscle of mice via adeno-associated viruses. Nat. Biomed. Eng. *4*, 97–110. https://doi.org/10.1038/s41551-019-0501-5.

58. Lim, C.K.W., McCallister, T.X., Saporito-Magriña, C., McPheron, G.D., Krishnan, R., Zeballos C, M.A., Powell, J.E., Clark, L.V., Perez-Pinera, P., and Gaj, T. (2022). CRISPR base editing of cis-regulatory elements enables the perturbation of neurodegeneration-linked genes. Mol. Ther. *30*, 3619–3631. https://doi.org/10.1016/J.YMTHE.2022.08.008.

59. Van Putten, M., Hulsker, M., Young, C., Nadarajah, V.D., Heemskerk, H., Van Der Weerd, L., 'T Hoen, P.A.C., Van Ommen, G.J.B., and Aartsma-Rus, A.M. (2013). Low dystrophin levels increase survival and improve muscle pathology and function in dystrophin/utrophin double-knockout mice. Faseb. J. *27*, 2484–2495. https://doi.org/10.1096/fj.12-224170.

60. Gonzalez, T.J., Simon, K.E., Blondel, L.O., Fanous, M.M., Roger, A.L., Maysonet, M.S., Devlin, G.W., Smith, T.J., Oh, D.K., Havlik, L.P., et al. (2022). Cross-species evolution of a highly potent AAV variant for therapeutic gene transfer and genome editing. Nat. Commun. *13*, 5947. https://doi.org/10.1038/s41467-022-33745-4.

61. El Andari, J., Renaud-Gabardos, E., Tulalamba, W., Weinmann, J., Mangin, L., Pham, Q.H., Hille, S., Bennett, A., Attebi, E., Bourges, E., et al. (2022). Semirational bioengineering of AAV vectors with increased potency and specificity for systemic gene therapy of muscle disorders. Sci. Adv. *8*, eabn4704. https://doi.org/10.1126/sciadv.abn4704.

62. Jackson, C.B., Richard, A.S., Ojha, A., Conkright, K.A., Trimarchi, J.M., Bailey, C.C., Alpert, M.D., Kay, M.A., Farzan, M., and Choe, H. (2020). AAV vectors engineered to target insulin receptor greatly enhance intramuscular gene delivery. Mol. Ther. Methods Clin. Dev. *19*, 496–506. https://doi.org/10.1016/j.omtm.2020.11.004.

63. Asokan, A., Conway, J.C., Phillips, J.L., Li, C., Hegge, J., Sinnott, R., Yadav, S., Diprimio, N., Nam, H.J., Agbandje-Mckenna, M., et al. (2010). Reengineering a receptor footprint of adeno-associated virus enables selective and systemic gene transfer to muscle. Nat. Biotechnol. *28*, 79–82. https://doi.org/10.1038/NBT.1599.

64. Pulicherla, N., Shen, S., Yadav, S., Debbink, K., Govindasamy, L., Agbandje-Mckenna, M., and Asokan, A. (2011). Engineering Liver-detargeted AAV9 Vectors for Cardiac and Musculoskeletal Gene Transfer. Mol. Ther. *19*, 1070–1078. https://doi.org/10.1038/MT.2011.22.

65. Elangkovan, N., and Dickson, G. (2021). Gene Therapy for Duchenne Muscular Dystrophy. J. Neuromuscul. Dis. *8*, S303–S316. https://doi.org/10.3233/JND-210678.

66. Brown, A., Woods, W.S., and Perez-Pinera, P. (2016). Multiplexed Targeted Genome Engineering Using a Universal Nuclease-Assisted Vector Integration System. ACS Synth. Biol. *5*, 582–588. https://doi.org/10.1021/acssynbio.6b00056.

67. Gapinske, M., Tague, N., Winter, J., Underhill, G.H., and Perez-Pinera, P. (2018). Targeted gene knock out using nuclease-assisted vector integration: Hemi- and Homozygous deletion of JAG1. In Methods in Molecular Biology (Humana Press Inc.), pp. 233–248. https://doi.org/10.1007/978-1-4939-7795-6_13.

68. Gaj, T., Epstein, B.E., and Schaffer, D.V. (2016). Genome engineering using Adeno-associated virus: Basic and clinical research applications. Mol. Ther. *24*, 458–464. https://doi.org/10.1038/mt.2015.151.

69. Clement, K., Rees, H., Canver, M.C., Gehrke, J.M., Farouni, R., Hsu, J.Y., Cole, M.A., Liu, D.R., Joung, J.K., Bauer, D.E., and Pinello, L. (2019). CRISPResso2 provides accurate and rapid genome editing sequence analysis. Nat. Biotechnol. *37*, 224–226. https://doi.org/10.1038/s41587-019-0032-3.

70. Dobin, A., Davis, C.A., Schlesinger, F., Drenkow, J., Zaleski, C., Jha, S., Batut, P., Chaisson, M., and Gingeras, T.R. (2013). STAR: ultrafast universal RNA-seq aligner. Bioinformatics *29*, 15–21. https://doi.org/10.1093/BIOINFORMATICS/BTS635.

71. Robinson, J.T., Thorvaldsdóttir, H., Winckler, W., Guttman, M., Lander, E.S., Getz, G., and Mesirov, J.P. (2011). Integrative genomics viewer. Nat. Biotechnol. *29*, 24–26. https://doi.org/10.1038/NBT.1754.

72. Santos, M.D., Gioftsidi, S., Backer, S., Machado, L., Relaix, F., Maire, P., and Mourikis, P. (2021). Extraction and sequencing of single nuclei from murine skeletal muscles. STAR Protoc. *2*, 100694. https://doi.org/10.1016/J.XPRO.2021.100694.

OMTN, Volume *33*

Supplemental information

Targeting Duchenne muscular dystrophy by skipping DMD exon 45 with base editors

Michael Gapinske, Jackson Winter, Devyani Swami, Lauren Gapinske, Wendy S. Woods, Shraddha Shirguppe, Angelo Miskalis, Anna Busza, Dana Joulani, Collin J. Kao, Kurt Kostan, Anne Bigot, Rashid Bashir, and Pablo Perez-Pinera

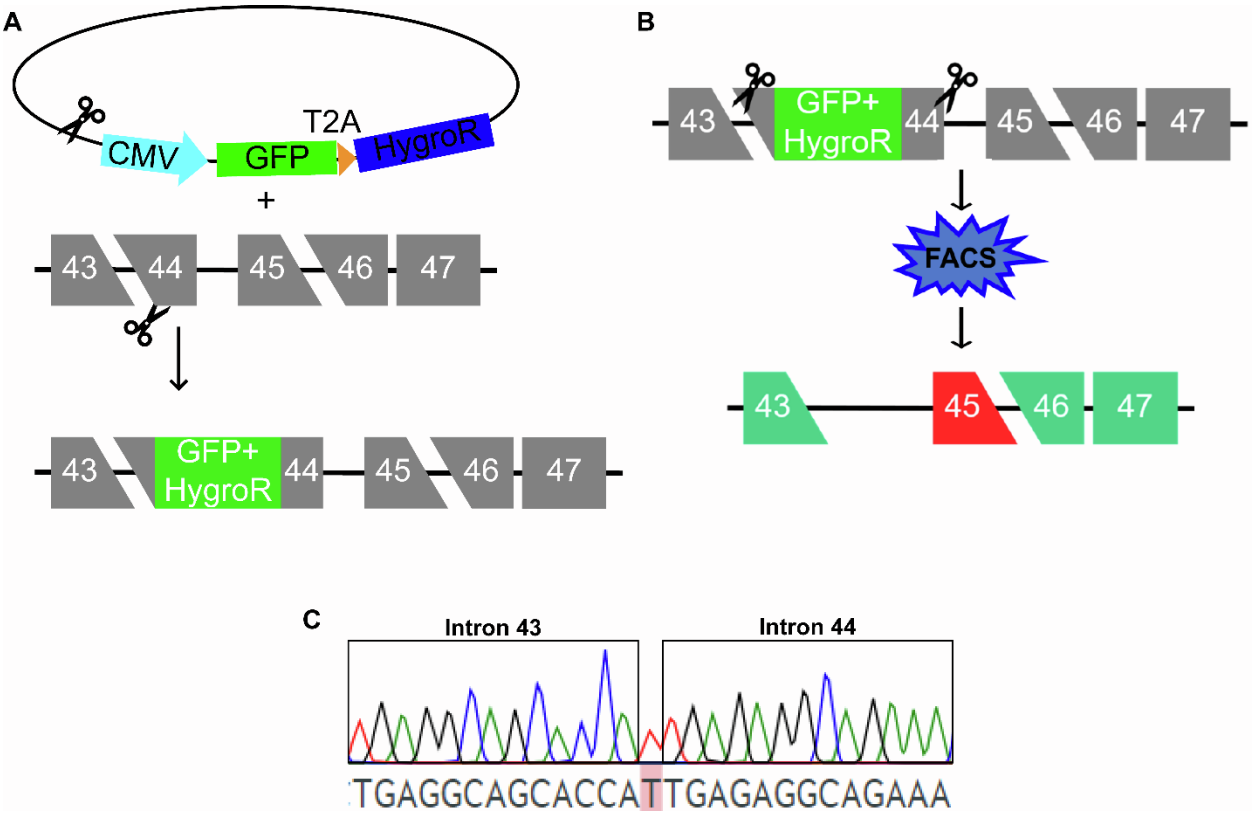

Figure S1. Strategy for creating Duchenne muscular dystrophy model cell lines. Nuclease Assisted Vector Integration was utilized to create a cell line with a deletion of *DMD* exon 44. Cells were co-transfected with active SpCas9, a transfer vector encoding a hygromycin resistance gene tethered to GFP via a T2A self-cleaving peptide, an sgRNA targeting the transfer vector, and an sgRNA targeting *DMD* exon 44. When SpCas9 causes simultaneous DSBs in the transfer vector and genome, the transfer vector can be integrated at the exon 44 target site **(A)**. Following clonal isolation with hygromycin, cells were re-transfected with SpCas9 and two sgRNAs targeting the introns flanking exon 44, and GFP-negative cells were isolated by FACS **(B)**. A clonal cell line with a deletion of exon 44 was isolated from this population, and Sanger sequencing confirmed a deletion from the intron 43 sgRNA cut site to the intron 44 cut site with the insertion of one T.

		EXON 45											
AA Sequence		E			L			Q			D		
DNA Sequence		G	A	A	C	T	C	C	A	G	G	A	T
DMDΔ44	A	0.02	100.00	100.00	0.00	0.00	0.00	0.00	100.00	0.00	0.01	99.98	0.00
	C	0.00	0.00	0.00	99.99	0.00	100.00	99.99	0.00	0.00	0.00	0.00	0.00
	G	99.98	0.00	0.00	0.00	0.00	0.00	0.00	0.00	99.99	99.99	0.02	0.00
	T	0.00	0.00	0.00	0.01	100.00	0.00	0.01	0.00	0.01	0.00	0.00	100.00
FNLS-Blast	A	0.26	99.98	100.00	0.00	0.00	0.00	0.00	100.00	0.00	0.03	99.94	0.00
	C	0.00	0.00	0.00	100.00	0.00	99.98	100.00	0.00	0.00	0.00	0.00	0.00
	G	99.74	0.02	0.00	0.00	0.00	0.00	0.00	0.00	100.00	99.97	0.04	0.00
	T	0.00	0.00	0.00	0.00	100.00	0.02	0.00	0.00	0.00	0.00	0.02	100.00
ABERA-Blast	A	0.00	99.86	99.84	0.01	0.00	0.00	0.01	99.93	0.00	0.02	99.97	0.00
	C	0.01	0.00	0.00	99.99	0.03	99.97	99.96	0.00	0.00	0.00	0.00	0.00
	G	99.95	0.12	**0.16**	0.00	0.00	0.00	0.00	0.02	100.00	99.98	0.01	0.01
	T	0.04	0.01	0.00	0.00	99.97	0.03	0.02	0.05	0.00	0.00	0.01	99.99

Figure S2. NGS Sequencing of *DMD* exon 45. IGVtools count of RNA-Seq base calls at the first 12 bases of *DMD* exon 45. Orange Highlight: ABE sgRNA PAM sequence. Red text: $p<0.001$; two-tailed unpaired t-test of each base; n=3.

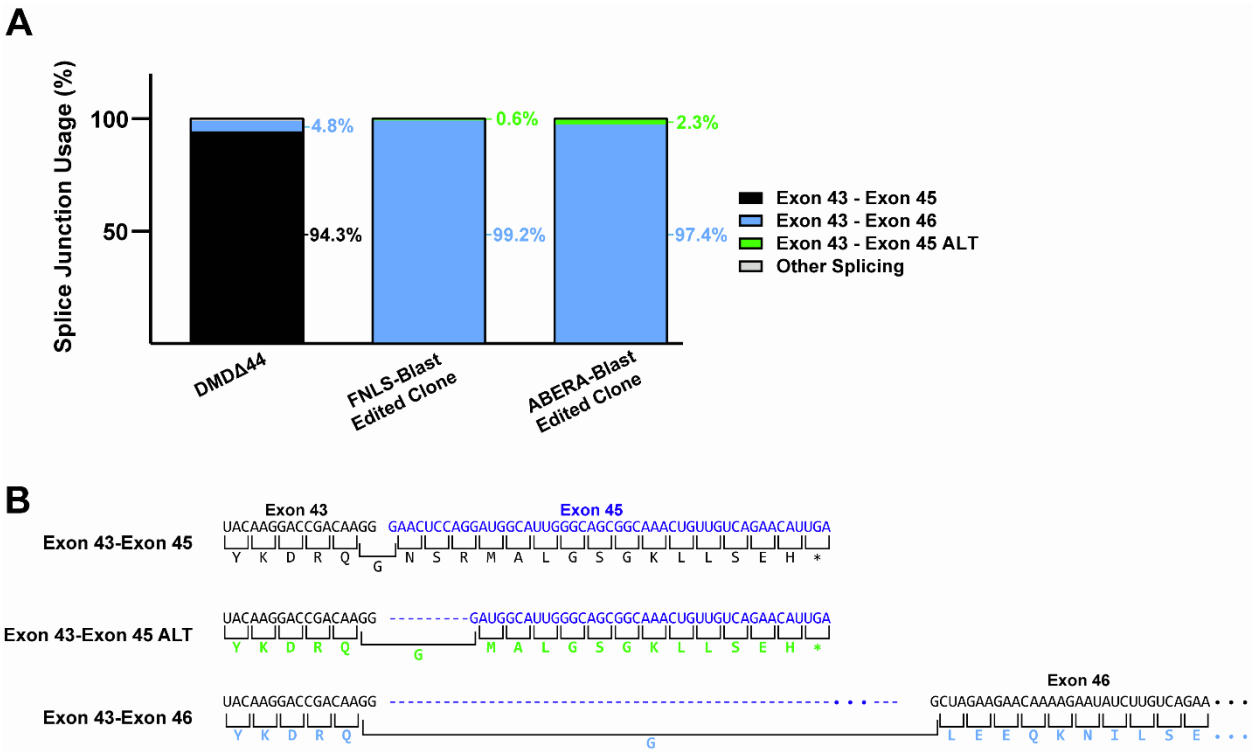

Figure S3. Splice junction usage in engineered skeletal muscle tissues from DMDΔ44 and corrected cell lines. **(A)** Part-of-whole graphs from RNA-Seq data representing the percentage of transcripts using the exon 43 splice donor and a given splice acceptor. Values plotted represent the mean percent-splice junction usage, n=3. **(B)** RNA and amino acid sequences resulting from each common splice event. A premature STOP codon results from the Exon 43-Exon 45 and the Exon 43-Exon 45 ALT splice junctions, however the Exon 43-Exon 46 splice junction recovers the reading frame.

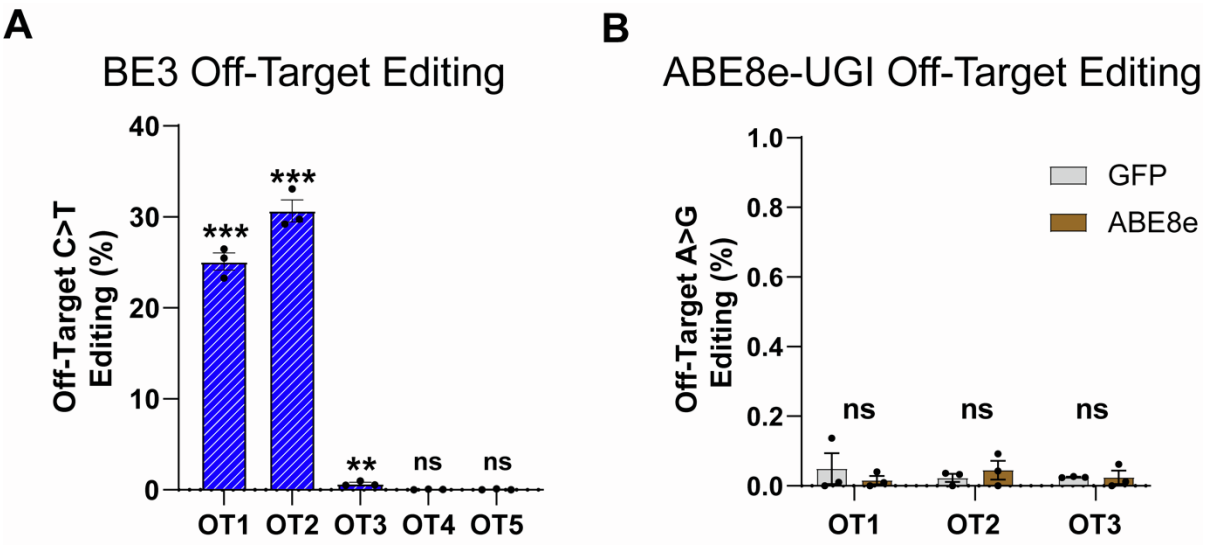

Figure S4. Off-target editing by split base editors. **(A)** BE3 produced substantial off-target editing at OT1 (25.1%) and OT2 (30.68%), as well as editing at OT3 (0.69%). No editing was seen at OT4 or OT5, the two highest-scoring off-target sites in coding regions. Each off-target site with a score above 2.0 was sequenced (OT1, OT2, and OT3), as well as the top two off-target sites found in intragenic sequences (OT4, XIST, and OT5, SCARF1). **(B)** No significant off-target editing was detected at any of the three off-target sites assigned a score greater than 2.0 by Benchling.com,[1] when using ABE8e and the *DMD* exon 45 targeting 20-base pair sgRNA. We tested the off-target editing rates at off-target sites predicted by Benchling.com using the algorithm of Hsu et al (2013).[1] Locations of tested sites are listed in **Table S1**. The highest editing rate detected at each off-target site is reported. Each off-target site with a score above 2.0 was sequenced. ns, not significant; two-tailed unpaired t-test compared to GFP-transfected control samples, n=3.

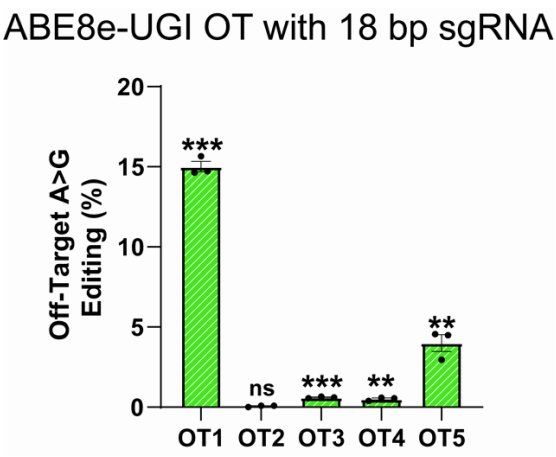

Figure S5. ABE8e off-target editing rates with an 18-nucleotide sgRNA spacer. The ABE8e-UGI with an 18-nucleotide sgRNA spacer edited non-coding off-target sites OT1, OT3, OT4 (15.0%, 0.61%, 0.51%) and off-target site OT5, which occurs in the 5' UTR of exon 1 of the SGO1 gene (4.0%). Each off-target site with a score above 5.0 was sequenced (OT1-4), as well as the top scoring intragenic off-target (OT5, SGO1). ns, not significant; **, $p<0.01$; ***, $p<0.001$; two-tailed unpaired t-test with compared to GFP-transfected control samples, n=3.

Table S1. List of tested sgRNA off-target sites.

Off-Target Designation	Off-Target Genomic Location (GRCh38)	Off-Target Score (Hsu et al, 2013)	Off-Target Gene
CBE OT1	chr13:+41675348	2.8	VWA8 (Intron) (ENSG00000102763)
CBE OT2	chr1:+209225724	2.4	Intergenic
CBE OT3	chr12:+14793350	2.2	WBP11 (Intron) (ENSG00000084463)
CBE OT4	chrX:+73833428	0.8	XIST (ENSG00000229807)
CBE OT5	chr17:+1635116	0.8	SCARF1 (ENSG00000074660)
ABE 18-base OT1	chr6:-119822211	92.1	Intergenic
ABE 18-base OT2	chr14:-52177038	5.7	Intergenic
ABE 18-base OT3	chr2:+26609282	61.1	CIB4 (Intron) (ENSG00000157884)
ABE 18-base OT4	chr17:-46875698	6.2	WNT9B (Intron) (ENSG00000158955)
ABE 18-base OT5	chr3:+20185983	3.9	SGO1 (ENSG00000129810)
ABE 20-base OT1	chr6:-119822211	4.2	Intergenic
ABE 20-base OT2	chr14:-52177038	3.6	Intergenic
ABE 20-base OT3	chr6:-40070568	2.5	Intergenic

Table S2. List of oligonucleotides used in this study.

Designation	Oligonucleotide Sequence
hDMD exon 45 CBE sgRNA sense oligo	CACCGTTCCTGTAAGATACCAAAA
hDMD exon 45 CBE sgRNA antisense oligo	AAACTTTTGGTATCTTACAGGAAC
hDMD exon 45 ABE 20-base sgRNA sense oligo	CACCGATCTTACAGGAACTCCAGGA
hDMD exon 45 ABE 20-base sgRNA antisense oligo	AAACTCCTGGAGTTCCTGTAAGATC
h/mDMD exon 45 ABE 18-base sgRNA sense oligo	CACCGCTTACAGGAACTCCAGGA
h/mDMD exon 45 ABE 18-base sgRNA antisense oligo	AAACTCCTGGAGTTCCTGTAAGC
Rosa26 control sgRNA sense oligo	CACCGCATGGATTTCTCCGGTGAAT
Rosa26 control sgRNA antisense oligo	AAACATTCACCGGAGAAATCCATGC
hDMD exon 44 integration sgRNA sense oligo	CACCGACAGATCTGTTGAGAAATGG
hDMD exon 44 integration sgRNA antisense oligo	AAACCCATTTCTCAACAGATCTGTC
Transfer vector integration sgRNA sense oligo	CACCGACCGGGTCTTCGAGAAGACC
Transfer vector integration sgRNA antisense oligo	AAACGGTCTTCTCGAAGACCCGGTC
Intron 43 deletion sgRNA sense oligo	CACCGCTCTGAGGCAGCACCATAGC
Intron 43 deletion sgRNA antisense oligo	AAACGCTATGGTGCTGCCTCAGAGC
Intron 44 deletion sgRNA sense oligo	CACCGTAATGGGGTTTCTGCCTGAG
Intron 44 deletion sgRNA antisense oligo	AAACCTCAGGCAGAAACCCCATTAC
hDMD exon 44 integration detection primer F	TACCTGCAGGCGATTTGACAGA
hDMD intron 44 integration detection primer R	CGATGCTTCCCTCTGTCACAGA
Transfer Vector integration detection primer	GGAGACTTGGAAATCCCCGTGA
Intron 43 deletion detection primer F	CCGGTGCCTGGCTATTAGTA
Intron 43 deletion detection primer R	TGCTTCATCGTAAAAGTACTCCCT
hDMD exon 45 gDNA Nextera Amp F	TCGTCGGCAGCGTCAGATGTGTATAAGAGACAGTGGAACATCCTTGTGGGGACAA
hDMD exon 45 gDNA Nextera Amp R	GTCTCGTGGGCTCGGAGATGTGTATAAGAGACAGTTCTGACAACAGTTTGCCGCTG
CBE OT1 gDNA Nextera Amp F	TCGTCGGCAGCGTCAGATGTGTATAAGAGACAGGTGTGCCGATTCCACCACATTTTAC
CBE OT1 gDNA Nextera Amp R	GTCTCGTGGGCTCGGAGATGTGTATAAGAGACAGCTTCTATATAACCAGATGTTTGTG GAGGAGTAAC
CBE OT2 gDNA Nextera Amp F	TCGTCGGCAGCGTCAGATGTGTATAAGAGACAGGCACAGAAGATTTTTAGGGCAGCT
CBE OT2 gDNA Nextera Amp R	GTCTCGTGGGCTCGGAGATGTGTATAAGAGACAGCACACAGCCTCCCCTGTTATCA
CBE OT3 gDNA Nextera Amp F	TCGTCGGCAGCGTCAGATGTGTATAAGAGACAGTGGTGTGCATTTTCCACTGTCA
CBE OT3 gDNA Nextera Amp R	GTCTCGTGGGCTCGGAGATGTGTATAAGAGACAGACAGGAAAGAAAGGAGAGTAGCCA
XIST gDNA Nextera Amp F	TCGTCGGCAGCGTCAGATGTGTATAAGAGACAGAGCAGTAGTAGCAGTTGCCACA
XIST gDNA Nextera Amp R	GTCTCGTGGGCTCGGAGATGTGTATAAGAGACAGTGCAGTCCTCAGGTCTCACATG

SCARF1 gDNA Nextera Amp F	TCGTCGGCAGCGTCAGATGTGTATAAGAGACAGGCCCTGTGACCACGATCTACAT
SCARF1 gDNA Nextera Amp R	GTCTCGTGGGCTCGGAGATGTGTATAAGAGACAGCCTGGGCTCTCCTTGAACTCTC
ABE OT1 gDNA Nextera Amp F	TCGTCGGCAGCGTCAGATGTGTATAAGAGACAGAGCTTGGTGTGAGACAGAGCAT
ABE OT1 gDNA Nextera Amp R	GTCTCGTGGGCTCGGAGATGTGTATAAGAGACAGGCATCTTCCACCTGTTTCTGCC
ABE OT2 gDNA Nextera Amp F	TCGTCGGCAGCGTCAGATGTGTATAAGAGACAGGCAAGGGTAGGGGTGAGACATT
ABE OT2 gDNA Nextera Amp R	GTCTCGTGGGCTCGGAGATGTGTATAAGAGACAGTGGGAGAATCACTTGAGCCCAG
ABE OT3 gDNA Nextera Amp F	TCGTCGGCAGCGTCAGATGTGTATAAGAGACAGTCCCAGAGCCCCAAATAAAGCA
ABE OT3 gDNA Nextera Amp R	GTCTCGTGGGCTCGGAGATGTGTATAAGAGACAGAACTCTCGGCCTCTTCACTGAC
ABE OT4 gDNA Nextera Amp F	TCGTCGGCAGCGTCAGATGTGTATAAGAGACAGCACGTCTTCAACCAGCATTCCC
ABE OT4 gDNA Nextera Amp R	GTCTCGTGGGCTCGGAGATGTGTATAAGAGACAGGGAGAAGTGGGCAGTTGCTCTA
SGOL1 gDNA Nextera Amp F	TCGTCGGCAGCGTCAGATGTGTATAAGAGACAGGGAAGCCGGAACATCTGAAAGC
SGOL1 gDNA Nextera Amp R	GTCTCGTGGGCTCGGAGATGTGTATAAGAGACAGGGAGAGCTTCGAAGAGCCTTGA
hDMD exon 41 RT-PCR F	CAGTGGAGCCAACTCAGATCCA
hDMD exon 47 RT-PCR R	TTGTTTGAGAATTCCCTGGCGC
hDMD exon 43 Nextera Amp RT-PCR F	TCGTCGGCAGCGTCAGATGTGTATAAGAGACAGCTACAGGAAGCTCTCTCCCAGC
hDMD exon 47 Nextera Amp RT-PCR R	GTCTCGTGGGCTCGGAGATGTGTATAAGAGACAGGCTCTTTTCCAGGTTCAAGTGGG

Table S3. Amino acid sequences of constructs cloned in previous publications.

Orange = NLS
Purple = EcTadA-derived adenine base editor domain
Blue = Linkers
Yellow Highlight = SpCas9-D10A
Red = UGI
Green Highlight = GFP
Underline = T2A
Brown = Hygromycin Resistance Gene

ABE7.10-GGGGS5-UGI[2]

MSEVEFSHEYWMRHALTLAKRAWDEREVPVGAVLVHNNRVIGEGWNRPIGRHDPTAHAEIMALRQGGL
VMQNYRLIDATLYVTLEPCVMCAGAMIHSRIGRVVFGARDAKTGAAGSLMDVLHHPGMNHRVEITEGILA
DECAALLSDFFRMRRQEIKAQKKAQSSTDSGGSSGGSSGSETPGTSESAT
PESSGGSSGGSSEVEFSHEYWMRHALTLAKRARDEREVPVGAVLVLNNRVIGEGWNRAIGLHDPTAHAEI
MALRQGGLVMQNYRLIDATLYVTFEPCVMCAGAMIHSRIGRVVFGVRNAKTGAAGSLMDVLHYPGMNH
RVEITEGILADECAALLCYFFRMPRQVFNAQKKAQSSTDASGGGGSGGGGSGGGGSGGGGSGGGGSGTDK
KYSIGLAIGTNSVGWAVITDEYKVPSKKFKVLGNTDRHSIKKNLIGALLFDSGETAEATRLKRTARRRYTRR
KNRICYLQEIFSNEMAKVDDSFFHRLEESFLVEEDKKHERHPIFGNIVDEVAYHEKYPTIYHLRKKLVDSTD
KADLRLIYLALAHMIKFRGHFLIEGDLNPDNSDVDKLFIQLVQTYNQLFEENPINASGVDAKAILSARLSKS
RRLENLIAQLPGEKKNGLFGNLIALSLGLTPNFKSNFDLAEDAKLQLSKDTYDDDLDNLLAQIGDQYADLF
LAAKNLSDAILLSDILRVNTEITKAPLSASMIKRYDEHHQDLTLLKALVRQQLPEKYKEIFFDQSKNGYAGY
IDGGASQEEFYKFIKPILEKMDGTEELLVKLNREDLLRKQRTFDNGSIPHQIHLGELHAILRRQEDFYPFLKD
NREKIEKILTFRIPYYVGPLARGNSRFAWMTRKSEETITPWNFEEVVDKGASAQSFIERMTNFDKNLPNEKV
LPKHSLLYEYFTVYNELTKVKYVTEGMRKPAFLSGEQKKAIVDLLFKTNRKVTVKQLKEDYFKKIECFDSV
EISGVEDRFNASLGTYHDLLKIIKDKDFLDNEENEDILEDIVLTLTLFEDREMIEERLKTYAHLFDDKVMKQL
KRRRYTGWGRLSRKLINGIRDKQSGKTILDFLKSDGFANRNFMQLIHDDSLTFKEDIQKAQVSGQGDSLHE
HIANLAGSPAIKKGILQTVKVVDELVKVMGRHKPENIVIEMARENQTTQKGQKNSRERMKRIEEGIKELGS
QILKEHPVENTQLQNEKLYLYYLQNGRDMYVDQELDINRLSDYDVDHIVPQSFLKDDSIDNKVLTRSDKN
RGKSDNVPSEEVVKKMKNYWRQLLNAKLITQRKFDNLTKAERGGLSELDKAGFIKRQLVETRQITKHVAQ
ILDSRMNTKYDENDKLIREVKVITLKSKLVSDFRKDFQFYKVREINNYHHAHDAYLNAVVGTALIKKYPKL
ESEFVYGDYKVYDVRKMIAKSEQEIGKATAKYFFYSNIMNFFKTEITLANGEIRKRPLIETNGETGEIVWDK
GRDFATVRKVLSMPQVNIVKKTEVQTGGFSKESILPKRNSDKLIARKKDWDPKKYGGFDSPTVAYSVLVV
AKVEKGKSKKLKSVKELLGITIMERSSFEKNPIDFLEAKGYKEVKKDLIIKLPKYSLFELENGRKRMLASAG
ELQKGNELALPSKYVNFLYLASHYEKLKGSPEDNEQKQLFVEQHKHYLDEIIEQISEFSKRVILADANLDKV
LSAYNKHRDKPIREQAENIIHLFTLTNLGAPAAFKYFDTTIDRKRYTSTKEVLDATLIHQSITGLYETRIDLSQ
LGGDSRADSGGSTNLSDIIEKETGKQLVIQESILMLPEEVEEVIGNKPESDILVHTAYDESTDENVMLLTSDA
PEYKPWALVIQDSNGENKIKMLSGGSPKKKRKV*

pCMV-GFP-T2A-HygroR[3]

MGSVSKGEELFTGVVPILVELDGDVNGHKFSVSGEGEGDATYGKLTLKFICTTGKLPVPWPTLVTTLTYGV
QCFSRYPDHMKQHDFFKSAMPEGYVQERTIFFKDDGNYKTRAEVKFEGDTLVNRIELKGIDFKEDGNILGH
KLEYNYNSHNVYIMADKQKNGIKVNFKIRHNIEDGSVQLADHYQQNTPIGDGPVLLPDNHYLSTQSALSK
DPNEKRDHMVLLEFVTAAGITLGMDELYKTGPWEGRGSLLTCGDVEENPGPEFMAKKPELTATSVEKFLIE
KFDSVSDLMQLSEGEESRAFSFDVGGRGYVLRVNSCADGFYKDRYVYRHFASAALPIPEVLDIGEFSESLTY
CISRRAQGVTLQDLPETELPAVLQPVAEAMDAIAAADLSQTSGFGPFGPQGIGQYTTWRDFICAIADPHVYH
WQTVMDDTVSASVAQALDELMLWAEDCPEVRHLVHADFGSNNVLTDNGRITAVIDWSEAMFGDSQYEV
ANIFFWRPWLACMEQQTRYFERRHPELAGSPRLRAYMLRIGLDQLYQSLVDGNFDDAAWAQGRCDAIVR
SGAGTVGRTQIARRSAAVWTDGCVEVLADSGNRRPSTRPRAKE*

Table S4. Amino acid sequences of lentiviral base editor constructs used in this study.

Green = Flag Epitope Tag
Orange = NLS
Purple = Nucleobase deaminase (APOBEC1 or EcTadA-derived adenine base editor domain)
Blue = Linkers
Yellow Highlight = SpCas9-D10A
Red = UGI
Underline = P2A
Brown = Blasticidin resistance gene

pLenti-EFS-FNLS-P2a-BlastR

MDYKDHDGDYKDHDIDYKDDDDKMAPKKKRKVGIHGVPAAMSSETGPVAVDPTLRRRIEPHE
FEVFFDPRELRKETCLLYEINWGGRHSIWRHTSQNTNKHVEVNFIEKFTTERYFCPNTRCSITWFL
SWSPCGECSRAITEFLSRYPHVTLFIYIARLYHHADPRNRQGLRDLISSGVTIQIMTEQESGYCWR
NFVNYSPSNEAHWPRYPHLWVRLYVLELYCIILGLPPCLNILRRKQPQLTFFTIALQSCHYQRLPP
HILWATGLKSGSETPGTSESATPESDKKYSIGLAIGTNSVGWAVITDEYKVPSKKFKVLGNTDRH
SIKKNLIGALLFDSGETAEATRLKRTARRRYTRRKNRICYLQEIFSNEMAKVDDSFFHRLEESFLV
EEDKKHERHPIFGNIVDEVAYHEKYPTIYHLRKKLVDSTDKADLRLIYLALAHMIKFRGHFLIEG
DLNPDNSDVDKLFIQLVQTYNQLFEENPINASGVDAKAILSARLSKSRRLENLIAQLPGEKKNGLF
GNLIALSLGLTPNFKSNFDLAEDAKLQLSKDTYDDDLDNLLAQIGDQYADLFLAAKNLSDAILLS
DILRVNTEITKAPLSASMIKRYDEHHQDLTLLKALVRQQLPEKYKEIFFDQSKNGYAGYIDGGAS
QEEFYKFIKPILEKMDGTEELLVKLNREDLLRKQRTFDNGSIPHQIHLGELHAILRRQEDFYPFLK
DNREKIEKILTFRIPYYVGPLARGNSRFAWMTRKSEETITPWNFEEVVDKGASAQSFIERMTNFD
KNLPNEKVLPKHSLLYEYFTVYNELTKVKYVTEGMRKPAFLSGEQKKAIVDLLFKTNRKVTVK
QLKEDYFKKIECFDSVEISGVEDRFNASLGTYHDLLKIIKDKDFLDNEENEDILEDIVLTLTLFEDR
EMIEERLKTYAHLFDDKVMKQLKRRRYTGWGRLSRKLINGIRDKQSGKTILDFLKSDGFANRNF
MQLIHDDSLTFKEDIQKAQVSGQGDSLHEHIANLAGSPAIKKGILQTVKVVDELVKVMGRHKPE
NIVIEMARENQTTQKGQKNSRERMKRIEEGIKELGSQILKEHPVENTQLQNEKLYLYYLQNGRD
MYVDQELDINRLSDYDVDHIVPQSFLKDDSIDNKVLTRSDKNRGKSDNVPSEEVVKKMKNYWR
QLLNAKLITQRKFDNLTKAERGGLSELDKAGFIKRLVETRQITKHVAQILDSRMNTKYDENDKLI
REVKVITLKSKLVSDFRKDFQFYKVREINNYHHAHDAYLNAVVGTALIKKYPKLESEFVYGDYK
VYDVRKMIAKSEQEIGKATAKYFFYSNIMNFFKTEITLANGEIRKRPLIETNGETGEIVWDKGRDF
ATVRKVLSMPQVNIVKKTEVQTGGFSKESILPKRNSDKLIARKKDWDPKKYGGFDSPTVAYSVL
VVAKVEKGKSKKLKSVKELLGITIMERSSFEKNPIDFLEAKGYKEVKKDLIIKLPKYSLFELENGR
KRMLASAGELQKGNELALPSKYVNFLYLASHYEKLKGSPEDNEQKQLFVEQHKHYLDEIIEQISE
FSKRVILADANLDKVLSAYNKHRDKPIREQAENIIHLFTLTNLGAPAAFKYFDTTIDRKRYTSTKE
VLDATLIHQSITGLYETRIDLSQLGGDSGGSTNLSDIIEKETGKQLVIQESILMLPEEVEEVIGNKPE
SDILVHTAYDESTDENVMLLTSDAPEYKPWALVIQDSNGENKIKMLSGGSPKKKRKVMHSGSG
ATNFSLLKQAGDVEENPGPMHAKPLSQEESTLIERATATINSIPISEDYSVASAALSSDGRIFTGVN
VYHFTGGPCAELVVLGTAAAAAAGNLTCIVAIGNENRGILSPCGRCRQVLLDLHPGIKAIVKDSD
GQPTAVGIRELLPSGYVWEG*

pLenti-EFS-ABERA-P2a-BlastR

MDYKDDDDKMAPKKKRKVGIHGVPAASEVEFSHEYWMRHALTLAKRAWDEREVPVGAVLVH
NNRVIGEGWNRPIGRHDPTAHAEIMALRQGGLVMQNYRLIDATLYVTLEPCVMCAGAMIHSRIG
RVVFGARDAKTGAAGSLMDVLHHPGMNHRVEITEGILADECAALLSDFFRMRRQEIKAQKKAQ
SSTDSGGSSGGSSGSETPGTSESATPESSGGSSGGSSEVEFSHEYWMRHALTLAKRARDEREVPV
GAVLVLNNRVIGEGWNRAIGLHDPTAHAEIMALRQGGLVMQNYRLIDATLYVTFEPCVMCAGA
MIHSRIGRVVFGVRNAKTGAAGSLMDVLHYPGMNHRVEITEGILADECAALLCYFFRMPRQVFN
AQKKAQSSTDSGGSSGGSSGSETPGTSESATPESSGGSSGGSDKKYSIGLAIGTNSVGWAVITDEY
KVPSKKFKVLGNTDRHSIKKNLIGALLFDSGETAEATRLKRTARRRYTRRKNRICYLQEIFSNEM
AKVDDSFFHRLEESFLVEEDKKHERHPIFGNIVDEVAYHEKYPTIYHLRKKLVDSTDKADLRLIY
LALAHMIKFRGHFLIEGDLNPDNSDVDKLFIQLVQTYNQLFEENPINASGVDAKAILSARLSKSRR
LENLIAQLPGEKKNGLFGNLIALSLGLTPNFKSNFDLAEDAKLQLSKDTYDDDLDNLLAQIGDQY
ADLFLAAKNLSDAILLSDILRVNTEITKAPLSASMIKRYDEHHQDLTLLKALVRQQLPEKYKEIFF
DQSKNGYAGYIDGGASQEEFYKFIKPILEKMDGTEELLVKLNREDLLRKQRTFDNGSIPHQIHLG
ELHAILRRQEDFYPFLKDNREKIEKILTFRIPYYVGPLARGNSRFAWMTRKSEETITPWNFEEVVD
KGASAQSFIERMTNFDKNLPNEKVLPKHSLLYEYFTVYNELTKVKYVTEGMRKPAFLSGEQKKA
IVDLLFKTNRKVTVKQLKEDYFKKIECFDSVEISGVEDRFNASLGTYHDLLKIIKDKDFLDNEENE
DILEDIVLTLTLFEDREMIEERLKTYAHLFDDKVMKQLKRRRYTGWGRLSRKLINGIRDKQSGKT
ILDFLKSDGFANRNFMQLIHDDSLTFKEDIQKAQVSGQGDSLHEHIANLAGSPAIKKGILQTVKV
VDELVKVMGRHKPENIVIEMARENQTTQKGQKNSRERMKRIEEGIKELGSQILKEHPVENTQLQ
NEKLYLYYLQNGRDMYVDQELDINRLSDYDVDHIVPQSFLKDDSIDNKVLTRSDKNRGKSDNV
PSEEVVKKMKNYWRQLLNAKLITQRKFDNLTKAERGGLSELDKAGFIKRQLVETRQITKHVAQI
LDSRMNTKYDENDKLIREVKVITLKSKLVSDFRKDFQFYKVREINNYHHAHDAYLNAVVGTALI
KKYPKLESEFVYGDYKVYDVRKMIAKSEQEIGKATAKYFFYSNIMNFFKTEITLANGEIRKRPLIE
TNGETGEIVWDKGRDFATVRKVLSMPQVNIVKKTEVQTGGFSKESILPKRNSDKLIARKKDWDP
KKYGGFDSPTVAYSVLVVAKVEKGKSKKLKSVKELLGITIMERSSFEKNPIDFLEAKGYKEVKK
DLIIKLPKYSLFELENGRKRMLASAGELQKGNELALPSKYVNFLYLASHYEKLKGSPEDNEQKQL
FVEQHKHYLDEIIEQISEFSKRVILADANLDKVLSAYNKHRDKPIREQAENIIHLFTLTNLGAPAAF
KYFDTTIDRKRYTSTKEVLDATLIHQSITGLYETRIDLSQLGGDKRPAATKKAGQAKKKKASGSG
ATNFSLLKQAGDVEENPGPMHAKPLSQEESTLIERATATINSIPISEDYSVASAALSSDGRIFTGVN
VYHFTGGPCAELVVLGTAAAAAAGNLTCIVAIGNENRGILSPCGRCRQVLLDLHPGIKAIVKDSD
GQPTAVGIRELLPSGYVWEG*

Table S5. Amino acid sequences of adeno-associated viral base editor constructs used in this study.

Orange = NLS
Purple = Nucleobase deaminase (APOBEC1 or EcTadA-derived adenine base editor domain)
Blue = Linkers
Yellow Highlight = SpCas9-D10A
Red = UGI
Dark Green = N-RM Intein
Brown = C-RM intein
Underline = 3x HA tag

pAAV-CMV-N-ABE8e-DMD45

MKRTADGSEFESPKKKRKVSEVEFSHEYWMRHALTLAKRARDEREVPVGAVLVLNNRVIGEG
WNRAIGLHDPTAHAEIMALRQGGLVMQNYRLIDATLYVTFEPCVMCAGAMIHSRIGRVVFGVR
NSKRGAAGSLMNVLNYPGMNHRVEITEGILADECAALLCDFYRMPRQVFNAQKKAQSSINSGG
SSGGSSGSETPGTSESATPESSGGSSGGSDKKYSIGLAIGTNSVGWAVITDEYKVPSKKFKVLGNT
DRHSIKKNLIGALLFDSGETAEATRLKRTARRRYTRRKNRICYLQEIFSNEMAKVDDSFFHRLEES
FLVEEDKKHERHPIFGNIVDEVAYHEKYPTIYHLRKKLVDSTDKADLRLIYLALAHMIKFRGHFLI
EGDLNPDNSDVDKLFIQLVQTYNQLFEENPINASGVDAKAILSARLSKSRRLENLIAQLPGEKKN
GLFGNLIALSLGLTPNFKSNFDLAEDAKLQLSKDTYDDDLDNLLAQIGDQYADLFLAAKNLSDAI
LLSDILRVNTEITKAPLSASMIKRYDEHHQDLTLLKALVRQQLPEKYKEIFFDQSKNGYAGYIDG
GASQEEFYKFIKPILEKMDGTEELLVKLNREDLLRKQRTFDNGSIPHQIHLGELHAILRRQEDFYP
FLKDNREKIEKILTFRIPYYVGPLARGNSRFAWMTRKSEETITPWNFEEVVDKGASAQSFIERMTN
FDKNLPNEKVLPKHSLLYEYFTVYNELTKVKYVTEGMRKPAFLSGEQKKAIVDLLFKTNRKVTV
KQLKEDYFKKIECFDSVEISGVEDRFNASLGTYHDLLKIIKDKDFLDNEENEDILEDIVLTLTLFED
REMIEERLKTYAHLFDDKVMKQLKRRRYTGWGRLSRKLINGIRDKQSGKTILDFLKSDGFANRN
FMQLIHDDSLTFKEDIQKAQVCLAGDTLITLADGRRVPIRELVSQQNFSVWALNPQTYRLERARV
SRAFCTGIKPVYRLTTRLGRSIRATANHRFLTPQGWKRVDELQPGDYLALPRRIPTAS*

pAAV-CMV-C-ABE8e-UGI-DMD45

MAAACPELRQLAQSDVYWDPIVSIEPDGVEEVFDLTVPGPHNFVANDIIAHNSGQGDSLHEHIAN
LAGSPAIKKGILQTVKVVDELVKVMGRHKPENIVIEMARENQTTQKGQKNSRERMKRIEEGIKEL
GSQILKEHPVENTQLQNEKLYLYYLQNGRDMYVDQELDINRLSDYDVDHIVPQSFLKDDSIDNK
VLTRSDKNRGKSDNVPSEEVVKKMKNYWRQLLNAKLITQRKFDNLTKAERGGLSELDKAGFIK
RQLVETRQITKHVAQILDSRMNTKYDENDKLIREVKVITLKSKLVSDFRKDFQFYKVREINNYHH
AHDAYLNAVVGTALIKKYPKLESEFVYGDYKVYDVRKMIAKSEQEIGKATAKYFFYSNIMNFFK
TEITLANGEIRKRPLIETNGETGEIVWDKGRDFATVRKVLSMPQVNIVKKTEVQTGGFSKESILPK
RNSDKLIARKKDWDPKKYGGFDSPTVAYSVLVVAKVEKGKSKKLKSVKELLGITIMERSSFEKN
PIDFLEAKGYKEVKKDLIIKLPKYSLFELENGRKRMLASAGELQKGNELALPSKYVNFLYLASHY
EKLKGSPEDNEQKQLFVEQHKHYLDEIIEQISEFSKRVILADANLDKVLSAYNKHRDKPIREQAE
NIIHLFTLTNLGAPAAFKYFDTTIDRKRYTSTKEVLDATLIHQSITGLYETRIDLSQLGGDSGGSTN
LSDIIEKETGKQLVIQESILMLPEEVEEVIGNKPESDILVHTAYDESTDENVMLLTSDAPEYKPWA
LVIQDSNGENKIKMLSYPYDVPDYAYPYDVPDYAYPYDVPDYASGGSPKKKRKV*

Supplemental References

1. Hsu, P. D. *et al.* DNA targeting specificity of RNA-guided Cas9 nucleases. *Nat. Biotechnol.* **31**, 827–832 (2013).

2. Winter, J. *et al.* Targeted exon skipping with AAV-mediated split adenine base editors. *Cell Discov.* **5**, 1–12 (2019).

3. Brown, A., Woods, W. S. & Perez-Pinera, P. Multiplexed Targeted Genome Engineering Using a Universal Nuclease-Assisted Vector Integration System. *ACS Synth. Biol.* **5**, 582–588 (2016).